Techno-economic assessment of wine industry residue valorization: Distillation to bioethanol vs. Hydrothermal liquefaction to biofuels

MSc SET – Thesis project
EEMCS
SET 3901

2025
Rafael Martin Arroyo — 5153026

Declaration of Originality

I, Rafael Martin Arroyo, hereby declare that this thesis is the result of my own independent work. All sources of information, data, figures, and ideas taken from the work of others have been properly cited and acknowledged. This thesis has not been submitted for any degree or other qualification at any other academic institution.

Rafael Martín Arroyo
Delft University of Technology
Date: 21/11/2025

Abstract

The present work investigates the valorization of wine industry residues through the production of advanced biofuels, focusing on grape pomace as a representative lignocellulosic feedstock. The study aims to assess the technical and economic feasibility of converting this residue into liquid fuels via **hydrothermal liquefaction (HTL)** and to compare its performance against the **bioethanol based pathway** currently implemented by **Destilerías y Biorefinerías Zambrana, S.A.** in the Basque Country.

An initial **laboratory-scale HTL experiment** was conducted using the same grape pomace feedstock employed by Zambrana, providing essential compositional and yield data. Based on these experimental results, a **large-scale simulation** was developed in **Aspen Plus** to replicate the process under industrial conditions and enable a consistent comparison between the two pathways. The model was divided into four main stages: HTL reaction, phase separation, decomposition and hydrogenation, and final distillation, and parameterized using experimental data and literature sources, including ultimate and proximate analyses, GC–MS-derived compositions, and product yield distributions.

The findings reveal that the **Zambrana biorefinery pathway** exhibits superior economic performance, primarily due to its **multi product configuration**, which enables comprehensive valorization of all output streams. Its operating costs are also substantially lower when compared with those of the HTL route. Conversely, the **HTL pathway**, although technically feasible and capable of producing hydrocarbons compatible with jet fuel specifications, is constrained by **high operational expenditures**, driven most notably by hydrogen consumption during upgrading, which renders it economically unviable under current market conditions.

Overall, this work underscores the potential of integrating **HTL into circular bioeconomy frameworks** as an alternative route for wine industry residue valorization. Further research should focus on reducing hydrogen-related costs, optimizing catalysts and energy integration, and expanding the feedstock scope to include other winery byproducts such as grape lees and stalks to enhance the overall sustainability of the system.

Acknowledgements

I would like to begin by expressing my sincere gratitude to my academic supervisor, Dr. Luis Cutz, for their guidance, expertise, and continuous support through this entire project. His feedback and encouragement were essential in shaping the direction of this work.

I would also like to thank the members of my thesis committee, Dr. Wiebren de Jong and Dr. Mahinder Ramdin for their time, constructive feedback and valuable discussions.

My appreciation extends to Destilerías y Biorefinerías Zambrana, S.A. for giving me the opportunity to collaborate on this project and for providing access to industrial process information and resources. I am especially grateful to my company supervisor, Iñaki Isasi, for his mentorship, availability, and practical insights into biorefinery operations, which greatly enriched the applied dimension of this study. I am also grateful to Adolfo del Río for his valuable contributions to the technical aspects of the pathway. I would also like to thank Dr Kamal Pasha for his assistance with the Aspen plus simulation.

Moving beyond the academic and technical world, I have to thank my parents for giving me the opportunity to peruse this career path and for their continuous motivation and encouragement they have given me throughout this journey. I would also like to thank my sister for her company and for the music filled hours she spent playing the piano beside me while I worked at my desk. I also want to thank my girlfriend for all her support during all those late nights and for giving me the push to finish this, without her I would probably still be writing this thesis.

Finally, I would like to thank all my colleagues and friends who have accompanied me throughout this journey, from late night study sessions to endless laughs shared after exams, it has truly been an incredible experience.

Contents

Nomenclature

Abbreviation	**Definition**
CE	Circular Economy
AD	Anaerobic digestion
GP	Grape Pomace
FeGP	Fermented Grape Pomance
FrGP	Fresh Grape Pomance
OPEX	Operating Expenditure
CAPEX	Capital Expenditure
DEVEX	Development Expenditure
N	Nitrogen
P	Phosphorus
K	Potassium
HHV	Higher Heating Value
LCA	Life Cycle Assesment
GREET	Greenhouse gases, Regulated Emissions, and Energy use in Technologies
MAWL	Maximum Allowable Water Loading
SOP	Standard Operation Procedure
BOY	Bio-Oil product Yield
BCY	Biochar product Yield
AY	Aqueous product Yield
GY	Gas product Yield
SAF	Sustainable Aviation Fuel

List of Figures

List of Tables

Chapter 1

Introduction

1.1. Background: Circular economy principles and their relevance to the Wine Industry

The circular economy has emerged as a central framework for rethinking resource use in modern industrial systems, offering responses to the environmental and economic limitations of traditional linear production models. It promotes waste reduction, long term resource efficiency, and the continual recirculation of materials through reuse, recycling, and recovery. By encouraging industries to redesign processes and products so that resource value is maintained for as long as possible, the circular economy supports global sustainability objectives and has become a prominent reference point in contemporary policy and industrial strategy [1], [2]
In sectors such as winemaking, the potential for a circular economy is extremely high, given the amounts of organic residues generated during production. Grape pomace, wine lees, grape stems, and wastewaters, all these materials, considered wastes, could be revalorized with novel and innovative technologies. The conversion of these waste resources could result in the production of sustainable biofuels, thus addressing both waste disposal and renewable energy production [3].

The application of circular economy principles in the wine industry underscores the sector's capacity for innovation and its ongoing transition towards more sustainable production practices. This model enhances resource efficiency and mitigates environmental pressures by extending the value of materials that would otherwise be discarded. Through the transformation of residues into economically and environmentally beneficial products, the wine industry demonstrates how circular strategies can support sustainability objectives and contribute to long term sectoral resilience and growth [4].

1.2. Problem Statement: Challenges in residue management and biofuel production

In 2024, the wine industry reached a vineyard surface area of approximately 7.1 million hectares and a global wine production of 225.8 million hectoliters (22.58×10^9L) [5] [6]. Considering that roughly 1.8 kg of grapes are required per litre of wine and that for every 10 kg of grapes pressed, about 2.7 kg of biomass residues (mainly grape pomace) are generated, this corresponds to an estimated 11 million tonnes of solid residues produced worldwide in 2024 [7].

Improper disposal of these residues can lead to environmental issues such as soil and water contamination, greenhouse gas emissions, and local odor problems [5]. Existing management practices, however, only occasionally achieve full economic and environmental valorization of these byproducts, partly due to their early stage of research and technological development. This situation underscores the need for more sustainable and innovative treatment and utilization pathways [7].
At this present time, the wine market is seeing a great deal of growth, with a size valuation of USD 417.85 billion in 2020, and projected to grow at a compound annual growth rate (CAGR) of 6.4% from 2021 to 2028 [8]. Increased production results in the generation of large amounts of waste, thus making residue management even more challenging. Biorefinery technologies for advanced biofuels and bioethanol have evolved over time, but they tend to suffer instrumental restraints regarding their economic viability, operable scale, technological inefficiency, or lack of appropriate quality of various substrates [7]. The logistics associated with the collection and processing of residues from the wine industry therefore becomes more complex and diversified in nature, especially in regions where winemaking is rather decentralized and the disposal residues are scattered [5].

The formulation of techno-economic strategies for residue management and biofuel production must consider all possible alternatives to address the challenges faced by these sectors. Identification of optimum pathways in processing residues will significantly help develop economic feasibility, which in return, would provide huge value returns for the wine industry while contributing to the world's overall ecosystem sustainability. This research will bridge these knowledge gaps by suggesting specific but effective alternatives.

1.3. Objectives of the Study: Comparative Analysis of Biofuel Production Pathways

This study examines the conversion of winemaking residues into biofuels by analysing two distinct production pathways. The first pathway assesses the techno economic performance of producing bioethanol through fermentation and distillation. The second explores the potential for generating advanced biofuels, including sustainable aviation fuel (SAF), via hydrothermal liquefaction (HTL). Together, these routes provide a comparative basis for evaluating the technical viability and economic competitiveness of alternative strategies for valorizing grape pomace.

By conducting a comprehensive comparative analysis, the study seeks to identify the most efficient, and economically viable approach to valorizing these type of residues. To achieve this objective, the study addresses the following research questions:

1. What are the energy and resource requirements for biofuel production through fermentation/distillation and HTL generated from wine industry residues, and to what extent do these pathways differ in terms of efficiency and scalability?
2. How do the production cost and economic feasibility of the distillation and hydrothermal liquefaction pathways compare under similar operating conditions?
3. What are the key techno-economic and logistical barriers for scaling these processes, and which pathway offers greater economic viability for industrial applications?
4. How can the wine and biofuel industries incorporate these pathways into their operations to promote circular economy principles and achieve sustainability goals?

The first pathway, in association with Biorefinerías Zambrana [9], aims to study biorefinery processes for producing bioethanol, a renewable fuel with enormous potential for numerous applications in transportation, chemical and food industries [9]. This pathway aims at optimizing the conversion of residues like grape pomace and wine lees into bioethanol of high added value while assessing factors as process efficiency, energy consumption, and economic feasibility.

In the second pathway, hydrothermal liquefaction (HTL) was employed to convert grape pomace, supplied by Biorefinerías Zambrana, into biocrude. The laboratory scale HTL experiment was conducted to determine the distribution of product yields across the aqueous, organic (biocrude), biochar, and gaseous phases. These experimental results served as the basis for developing an Aspen Plus simulation model of the process.

Since the detailed feedstock characterization data were not available at the time of modelling, elemental and proximate composition values were obtained from relevant literature sources to complement the experimental findings.

The simulation was designed to replicate the laboratory process under industrial scale operating conditions, enabling a direct comparison with the existing distillation based biorefinery process at Zambrana. Subsequently, a biocrude upgrading section was modelled entirely in Aspen Plus, with the objective of maximizing the yield of biofuel products and assessing the technical feasibility, energy efficiency, and scale up potential of the HTL pathway for the valorization of wine industry residues.
To accomplish these research objectives, the study endeavors to do the following:

- Ascertain energy and resource requirements for each biofuel production process.
- Compare techno-economic aspects of each pathway under similar operating conditions.
- Define the key technical, financial, and logistical barriers affecting the scale up of each process and assess their likelihood for industrial implementation.
- Provide strategic recommendations on how to implement these valorization routes into the wine and biofuel sectors, embracing principles of the circular economy and long term sustainability.

1.4. Scope, boundaries and Limitations: Geographic, technical, and economic boundaries of the study

This study aims to evaluate the techno-economic feasibility of biofuel production from residues from the wine industry, with a specific focus on two distinct pathways. While the findings provide valuable insights into residue valorization, certain geographic, technical, and economic limitations must be acknowledged.

1.4.1. Geographic Limitations

The study focuses on the residues of the wine industry from the vinyards of La Rioja, in Spain, a region renowned worldwide for its quality wine (figure 1.1) [10]. The unique characteristics of the grape pomace residues from this region, influenced by local grape varieties, soil composition, and vinification practices, may differ from residues in other countries or continents [11]. Although the study aims to offer a global perspective for biofuel production, the findings may lack precision when extrapolated to other vineyards with different residue compositions.

Figure 1.1: Map of Spain and La rioja [12]

1.4.2. Technical Limitations

The first pathway, conducted in collaboration with Biorefinerías Zambrana, will leverage state of the art technology for bioethanol production. However, as the biorefinery plant is still under construction and planned to begin operations in Q1 2026, all data used for this pathway will be derived from simulations rather than operational processes.

The second pathway, hydrothermal liquefaction (HTL), was investigated using university scale experimental equipment that is less advanced from an industrial engineering standpoint. As a result, the work was carried out at laboratory scale, which inherently limits the direct applicability of the findings to large scale operations. The HTL experiments conducted at TU Delft employed the same grape pomace residues processed by Biorefinerías Zambrana, although the material had to be transported from Spain to the Netherlands. Such transport may introduce quality changes in the feedstock due to possible degradation during transit. These constraints highlight the dependence on small scale experimentation and process simulation, which cannot fully reproduce the operational dynamics of industrial HTL systems.

Seasonal Limitations

The timing of this study (Q1 of 2025) will impose certain seasonal limitations on the quality of the vine lees used in the TU Delft laboratory. Typically, La Rioja vineyards harvest grapes between August and October, which means that the lees available for this research were collected during the 2024 harvest season [13]. The lees and pomace, are not fresh and have undergone an extended ageing process as part of the winemaking procedure. As a result, their bioreactivity has decreased, potentially affecting their efficiency for biofuel production. This limitation highlights the importance of the freshness of the residue in assessing its potential for valorization.

In summary, these limitations establish the parameters within which the study functions, as well as guide realistic expectations about the study's findings. Nonetheless, within this framework, the research strives to provide sound conclusions regarding the potential of residues from the wine industry to yield biofuels and would thus contribute to a broader goal of creating sustainability initiatives for both the wine and energy sectors.

1.4.3. Thesis Structure

This thesis is organized into seven main chapters, complemented by appendices:

Chapter 1 introduces the study by outlining the background, the problem statement, and the objectives. It further defines the geographic, technical, and economic boundaries of the work and provides an overview of the thesis structure.

Chapter 2 presents the literature review. It begins with global trends in circular economy principles and their application within agro industries, followed by a detailed examination of residue composition and current valorization practices in the wine sector. The chapter then establishes the conceptual framework for comparing biofuel production pathways, reviewing technological fundamentals for bioethanol production and hydrothermal liquefaction (HTL).

Chapter 3 describes Pathway 1: Bioethanol Production. It details the industrial process implemented at Biorefinerías Zambrana, including feedstock handling, fermentation, distillation, and byproduct management. The chapter concludes with the associated mass balance and economic evaluation.

Chapter 4 introduces Pathway 2: Hydrothermal Liquefaction (HTL) at the experimental scale. It outlines the laboratory setup at TU Delft, including equipment specifications, operating conditions, product collection, and primary separation steps. Analytical methods used for characterizing HTL products are also presented.

Chapter 5 extends the HTL pathway through process simulation and upgrading in Aspen Plus. It details the construction of the simulation environment, the definition of pseudocomponents, decomposition modeling, vapor–liquid and liquid–liquid separation stages, and the upgrading of the biocrude into biodiesel range products. The chapter concludes with the economic assessment of the HTL based route.

Chapter 6 presents the integrated results and discussion. It compares the yields, product characteristics, and economic performance of both pathways and includes a sensitivity analysis examining key parameters that influence overall process feasibility. The chapter concludes by outlining the main limitations of the study and proposing mitigation strategies.

Chapter 7 provides the conclusions and recommendations. It synthesizes the central findings, discusses their implications for industry and policymakers, and identifies opportunities for future research.

The appendices supply supplementary material, including detailed process data, extended analytical results, and supporting documentation.

Chapter 2

Literature Review

2.1. Circular Economy in Agro industries: Global Trends and Applications

The topic of a circular economy (CE) stands out as a crucial pilar to enhance environmental sustainability and resource efficiency across industries throughout all sectors [14]. In agro industries, the use of CE principals aims to reduce waste, maximize resource use and enforce close loop systems consistent with global sustainability goals [5].

2.1.1. Global Trends in Circular Economy for Agro industries

Agro industries, including sectors such as agriculture, food processing, and beverage production, generate substantial amounts of organic waste [15]. According Toufeix et al. [16] and the United Nations Environment Program (UNEP), food processing waste alone accounts for an estimate of 931 million tons annually. In the recent years there has been a significant rise in attempts to pursue CE practices in the stated sectors, primarily due to the rising population, and therefore waste, global policies with special focus on greener and sustainable practices, economic incentives, and consumer demands for more "eco friendly" products [15].
Key global trends include:

- **Policy driven Initiatives:** Governments and international organizations have enacted policies to encourage waste reduction and recycling in agro industries. Examples include the European Union's Farm to Fork strategy [14], which promotes sustainable food systems, and the Sustainable Development Goals (SDGs) of the United Nations, particularly Goal 12 on responsible consumption and production [17].

- **Technological Innovations:** Advances in biotechnology, and waste to energy technologies have enabled more efficient resource use and recovery. Innovations such as anaerobic digestion [18], pyrolysis [19], and enzymatic hydrolysis [20] are increasingly being used to convert agricultural residues into revalorized products such as biofuels and fertilizers.

- **Market Transformation:** Trends in consumer preferences have been changing drastically during the last decade. Consumers are now looking for sustainable and eco friendly products that align with their values. Brands are now adopting circular economy principles to meet these demands, such as creating biodegradable packaging or creating recycling plans to treat products at the end stage.

2.1.2. Applications of Circular Economy in Agro industries

Waste management, resource recovery, and the production of value added products are areas under which circular economy principles find practical applications in agro industries. Here are some notable examples:

Waste Management

Effective waste recovery is a key practice of CE in the agro industry. By adopting strategies such as waste segregation, composting, and controlled disposal, companies can minimize environmental impacts and external costs associated with them, as well as add new revenue streams from the revalorized waste product.

- **Composting and Soil Amendment:** Agricultural residues, such as crop stalks and fruit peels, are increasingly being composted to produce nutrient rich soil amendments. This practice is particularly prevalent in coffee and citrus industries [21]. In small farms, composting is often used as the main source of fuel due to the amount of biogas (mainly methane) generated.

- **Biogas Production:** Organic waste from agro industries, including dairy and meat processing plants, serves as feedstock for biogas plants. The resulting biogas is utilized for energy generation, while digestate is used as valuable organic fertilizer [22].

Resource Recovery and Recycling
Resource recovery transforms agro industrial residues into valuable secondary materials. Examples include:

- **Water Recycling:** Water intensive agro industries, such as sugar processing, textile or fruit and vegetable processing, implement technologies and strategies to recycle and reduce process water use, significantly reducing freshwater consumption [23].
- **Nutrient Recovery:** Technologies like Struvite precipitation extract nutrients from waste water, converting them into fertilizers, enhancing soil fertility and reducing the need for chemical fertilizers [24][25].

Value added Products
One of the most promising aspects of CE is the creation of value added products from agro industrial residues. Examples include:

- **Bio based Materials:** Residues from crops, such as wheat straw and rice husks, are converted into bio plastics or sustainable construction materials through a series of chemical processes [26] [27] [28].
- **Biochar Production:** Pyrolysis of agricultural residues can produce biochar, a carbon rich material that improves soil health and sequesters carbon, contributing to climate change mitigation [29][30]. Biochar can also be used as an alternative to coal in some processes, producing a carbon neutral cycle.
- **Biofuels:** Lignocellulosic biomass from agricultural waste can be processed into different types of biofuels through a multitude of chemical process (pyrolisis, HTL...), providing renewable energy alternatives with net (or close to) zero emissions [31] .
- **Nutraceuticals and Pharmaceuticals:** Waste products like grape pomace and fruit seeds are rich in bioactive compounds, such as; Polyphenols, phenolic acids, bioactive peptides, polysaccharides etc... All these compounds can be extracted and later used in health supplements and cosmetics [32] [33] [34] [35].

Looking into the future, it is clear that circular economies will provide immense benefits and significant opportunities for agro industries and industries across all sectors, in particular when focusing on innovation and sustainable practices. With the adoption of CE principles, these industries will open up new, creative avenues for the utilization of residues while contributing to much broader and more significant environmental and economic ends [36].

2.2. Wine Industry Residues: Composition and Current Valorization Strategies

The wine industry is a significant contributor to global agricultural production, generating substantial residues during the winemaking process. Approximately 20-25% of the total grape weight processed is left as residue after wine production [37] . These residues, if not managed properly, can pose environmental challenges but also offer opportunities for valorization within a circular economy framework.

The wine industry is an important component of global agricultural production, generating large amounts of residues during grape picking and the winemaking process. During winemaking, approximately 20-25% of the total grape weight is discarded as residual biomass [37]. Due to the nature of the residues, if they are not managed properly they may cause environmental problems, such as odors or pests. At the same time, through circular economy practices, these residues offer the opportunity to be revalorized for a revenue stream while mitigating the environmental problems.

2.2.1. Types of Residues in the Wine Industry

The wine industry generates a variety of biomass residues beyond grape pomace, including: fermentation lees, grape stems, wastewater, and other byproducts. Each presents unique challenges and opportunities for valorization [38]. According to Martinez et al. these residues can be described as follows [38]:

- **Grape Pomace:** This waste consists of the grape skin, seeds, and the pulp of the grapes after pressing. The composition of pomace varies considerably from grape variety and winemaking process, representing 15-40% of the weight of the grape itself. In white wines, pomace is fresh and sweet, while in red grape pomace it contains larger amounts of alcohol as a result of fermentation. Uses of grape pomace include animal feeding, composting, bioactive compound extraction, or biofuel production [38].

- **Fermentation Lees:** These are sediments that accumulate at the bottom of fermentation tanks during the winemaking process. Lees consist of organic acids, proteins, yeast, bacteria, and other insoluble compounds such as tartaric acid salts and polymerized tannins. While these residues can be challenging to manage, their high organic content makes them suitable for composting or potential extraction of valuable compounds [38].

- **Grape Stems:** Grape stems are the wooden parts that hold grape clusters together and connect them to the vine. They constitute approximately 3-7% of the total grape cluster weight and are primarily composed of water and lignified plant material. Stems have a high tannin content, which can produce a bitter taste if not removed during vinification. Valorization opportunities include using stems in bioenergy production or as a source of lignocellulosic material for composite materials [38].

- **Wastewater:** The winemaking process generates substantial volumes of wastewater, primarily derived from cleaning operations and cooling systems rather than direct product formulation [38]. Water consumption in wineries is highly seasonal, with approximately 60% of the total usage concentrated in the three months following harvest, when grapes are transformed into wine [38]. Significant regional disparities exist in water efficiency: Spanish wineries, for instance, consume between 3 and 6 litres of water per litre of wine produced, compared to approximately 1 litre in countries such as Italy and France [38]. This inefficiency results in up to 500% higher wastewater generation, leading to increased treatment costs and oversized wastewater treatment facilities.

- **Other Residues:** Additional residues and contaminants include carbon dioxide (CO_2) and sulfur compounds generated during the fermentation and stabilization processes.

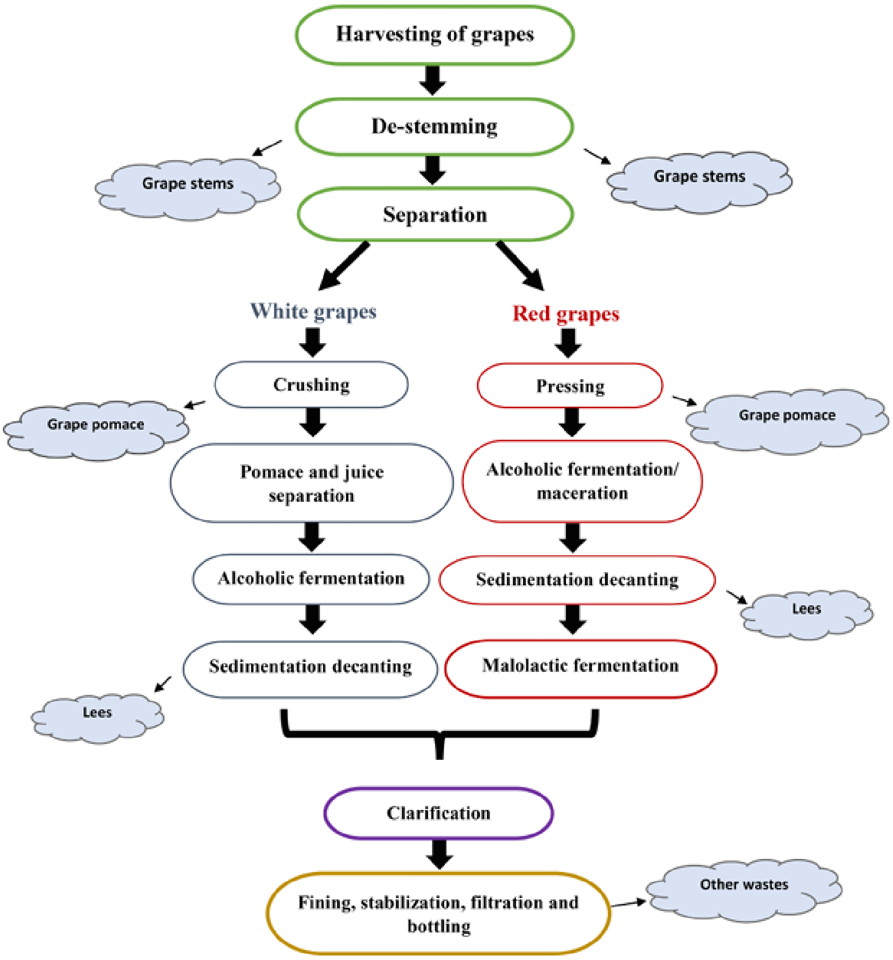

Figure 2.1: By products of the wine industry [39]

2.2.2. Composition of Grape Pomace

Grape pomace, the primary by product of winemaking, consists of skins, seeds, and stems. Its exact composition varies depending on factors such as grape variety, cultivation conditions, and winemaking processes [37], [40]. This variability is particularly evident when comparing fresh grape pomace (FrGP), derived from white wine production, with fermented grape pomace (FeGP), produced during red wine fermentation [41].

Figure 2.2: Dry grape pomace from red wine (A) and white wine (B) production [42]

The composition of grape pomace varies according to the type of grape used and therefore the winemaking process. For white winemaking, only the grape juice undergoes the fermentation process, leaving unused the fresh grape pomace (FrGP), which consists of skins, seeds and the stems of the grape clusters [41]. On the other hand, during the process of producing red wine, the solid components inside the pomace remain in contact during the fermentation process, producing a residue of fermented grape pomace (FeGP) [41]. The different grape treatments result in different physiochemical characteristics between the grape types. FeGp typycally contains lower levels of water soluble carbohydrates (WSC) while in FrGP these are largely metabolized by yeast during the fermentation process [41].

Table 2.1 presents the chemical composition of FeGP and FrGP collected in 2007 from Sutter Home Winery (St. Helena, Napa, CA, USA) [41]. The data highlights notable differences in key components such as lignin, cellulose, hemicellulose, and protein, which directly impact their suitability for various biofuel production pathways.

Table 2.1: Chemical Composition of Grape Pomace[a]

Chemical Component	FeGP (wt %, dry basis)	FrGP (wt %, dry basis)
Cellulose	14.5	9.2
Hemicellulose	10.3	4.0
Pectin	5.4	5.70
Lignin	17.2	11.6
Protein	14.5	7.0
WSC	2.7	49.1
Ash	8.0	12.6
Total C	48.2	44.3
Total N	2.5	1.2

[a] Both FeGP and FrGP were collected in 2007, and the as received moisture contents were 66.4% and 65.5%, respectively [41].

These compositional characteristics are critical for determining the optimal biofuel production process. FeGP, with its higher lignin and cellulose content, may be more suited for processes requiring lignocellulosic feedstocks, while the higher WSC content of FrGP makes it a better candidate for fermentation based pathways.

2.2.3. Current Valorization Strategies

Traditionally, grape pomace has been utilized in several ways, each offering unique benefits and applications. These valorization strategies are described in detail below:

1. **Animal Feed**: Grape pomace is commonly used as a feed supplement for livestock due to its high fiber and protein content [38] [43]. However, its use requires careful consideration of tannin levels, as excessive tannins can reduce digestibility [43] [44].

2. **Fertilizers and Soil Amendments**: One of the benefits of composting grape pomace is its ability to enhance soil quality by increasing the soil organic matter, improving soil stability and increasing nutrient availability. By composting, the overall volume for grape pomace is reduced and the organic content is stabilized, mitigating most of the environmental issues that would rise if left to decompose naturally.

3. **Distillation**: Grape pomace is used as a raw material for distilling alcoholic beverages such as grappa, a traditional spirit in Italy, or orujo in Spain [38]. This process involves fermenting the residual sugars in pomace, followed by distillation to extract alcohol (ethanol) [45]. The resulting distilled product has cultural and economic significance in many wine producing regions [46].

4. **Extraction of Bioactive Compounds**: Grape pomace is a rich source of phenolic compounds, flavonoids, anthocyanins, and tannins, which have strong antioxidant, anti inflammatory, and antimicrobial properties [40] [47] [35]. These bioactive compounds are widely used in the food, pharmaceutical, and cosmetic industries [48] [35]. Techniques such as supercritical fluid extraction, ultrasound assisted extraction, and solvent based methods are employed to isolate these valuable compounds efficiently [47] [48].

5. **Biofuel Production**: Advanced technologies like hydrothermal liquefaction (HTL) and pyrolysis can convert grape pomace into bio crude oil, biochar, and syngas, providing renewable energy solutions [49] [50]. HTL, in particular, operates under subcritical water conditions, breaking down the lignocellulosic matrix into liquid biofuels [51] [52]. This process eliminates the need for drying the biomass, making it energy efficient and suitable for wet feedstocks like grape pomace [51] [50].

6. **Nutraceuticals**: The development of nutraceuticals and functional foods from grape pomace is gaining traction due to its health benefits [53]. Grape pomace extracts, rich in polyphenols and dietary fibers, have been incorporated into bakery products, beverages, and dietary supplements [53] [54]. These products appeal to health conscious consumers and address the growing demand for natural, plant based ingredients [55].

7. **Biopolymers**: The use of grape pomace to produce biodegradable plastics offers a sustainable alternative to petroleum based polymers [56]. The lignin and cellulose in the pomace can be used as raw materials for bioplastics [57]. These materials are used in packaging, agricultural films, and disposable cutlery, aligning with global efforts to reduce plastic waste and promote a circular economy [58] [57].

Implementing these strategies requires investment in research and development, as well as collaboration between industry stakeholders to create efficient and sustainable processes.

2.3. Comparative Analyses in Biofuel Production: Methods and Framework

The conversion of biomass into biofuels is a fundamental component of sustainable energy systems and circular economy strategies. Biomass, a renewable and widely available resource, can be transformed into liquid and gaseous fuels such as bioethanol, biogas, biodiesel, and biocrude through a range of biorefinery processes [49]. These conversion routes are generally categorized into biological and thermochemical methods, each characterized by distinct reaction mechanisms, operating conditions, and product profiles [49]

2.3.1. Biological Conversion Pathways

Biological conversion pathways employ microorganisms and enzymatic reactions to transform biomass into fuels and bioproducts under relatively mild operating conditions [59]. These processes constitute an essential category of biomass valorization and provide context for bioethanol production, which is one of the pathways assessed in this study.

Anaerobic Digestion

Anaerobic digestion (AD) is a microbial process in which organic matter is degraded in the absence of oxygen, producing biogas composed mainly of methane (CH_4) and carbon dioxide (CO_2) [59] [49]. Although AD is widely applied for the treatment of agricultural residues and other wet organic wastes, it is not evaluated as part of the present study. Its inclusion here serves only to illustrate the broader spectrum of biological conversion routes documented in the literature.

Fermentation

Fermentation converts fermentable sugars into ethanol through the metabolic activity of microorganisms, most commonly Saccharomyces cerevisiae [60] [49]. This process forms the technological basis for industrial bioethanol production from sugar rich feedstocks such as sugarcane, corn, and molasses. Lignocellulosic residues require pre treatment and hydrolysis prior to fermentation so that cellulose and hemicellulose can be converted into fermentable sugars [61].

In the context of this thesis, fermentation is not modeled directly. Instead, the analysis focuses on the downstream separation and purification stages implemented at Biorefinerías Zambrana for recovering ethanol from the fermented broth. The discussion of fermentation is therefore limited to establishing the technological background of the industrial process used in the reference biorefinery.

2.3.2. Thermochemical Conversion Pathways

Thermochemical processes involve the application of heat, pressure, and chemical reactions to convert biomass into energy dense fuels and chemicals [49].

Pyrolysis:

Pyrolysis involves the thermal decomposition of biomass in the absence of oxygen, resulting in three primary products: bio oil (liquid), biochar (solid), and syngas (gas) [62] [49]. The distribution of these products depends on process parameters such as temperature, heating rate, and residence time. Fast pyrolysis, conducted at temperatures between 400–600°C with short residence times, is optimized for bio oil production, whereas slow pyrolysis favors biochar yield [63] [62].

Bio oil from pyrolysis is a potential substitute for fossil derived fuels, but its high oxygen content and instability require upgrading [64]. Biochar, on the other hand, finds applications as a soil amendment and in carbon sequestration, while syngas can be used for heat and power generation [63] [64].

Gasification:

Gasification converts biomass into syngas, a mixture of hydrogen (H_2), carbon monoxide (CO), and methane (CH_4), through partial oxidation at high temperatures (700–1200°C) [65] [66]. The process involves three stages: drying, pyrolysis, and the gasification reaction itself [65]. Syngas can be used directly in power generation or as a feedstock to produce synthetic fuels and chemicals through processes like Fischer Tropsch synthesis [67].

Gasification offers flexibility in feedstock and end products but faces challenges such as high capital costs, tar formation, and the need for advanced syngas cleaning technologies [68].

Hydrothermal Liquefaction (HTL):

Hydrothermal liquefaction is a promising technology for converting wet biomass into biocrude oil under subcritical water conditions (250–374°C and 10–25 MPa) [49] [51]. Unlike other thermochemical methods, HTL eliminates the need for biomass drying, making it particularly efficient for feedstocks with high moisture content, such as algae, food waste, and agricultural residues [49] [50].

Biocrude produced through HTL has a high energy density and can be upgraded into transportation fuels [49]. Challenges associated with HTL include reactor design, scalability, and the treatment of the aqueous phase, which contains organic contaminants [49] [51].

2.3.3. Framework for Comparative Analysis

To assess the performance of the two conversion pathways, the comparative analysis framework focuses on parameters directly relevant to this study. These include energy efficiency, product yield and composition, process operability, and overall economic viability. The following subsections provide an in depth examination of bioethanol production and hydrothermal liquefaction, describing their underlying mechanisms, technological characteristics, and roles in the broader context of sustainable biofuel production.

2.4. Bio Ethanol Production: Current Technologies and Case Studies

Bioethanol production from waste biomass represents a sustainable and innovative approach that aligns with circular economy principles by valorizing agricultural and industrial residues [49]. Within the wine industry, by-products such as grape pomace, lees, and stalks can be efficiently utilized to recover or produce ethanol, contributing to waste minimization and renewable energy generation [69]. This section focuses on the technical processes, chemical mechanisms used for bioethanol recovery in winery integrated biorefineries.

2.4.1. Technical Process and Chemistry of Bio Ethanol Production from Winery Residues

In contrast to conventional lignocellulosic bioethanol production, where structural carbohydrates must first be hydrolysed into fermentable sugars, ethanol recovery from winery residues focuses on **extracting already formed ethanol** present in liquid by-products and partially fermented streams [70]. These include lees, low wine, and de-alcoholized pomace solutions, which contain ethanol or ethanol precursors generated during winemaking [71] [70].

The industrial process implemented at Biorefinerías Zambrana can be grouped into four streamlined stages:

1. **Primary Alcohol Recovery:** Ethanol present in liquid residues such as lees and low wine is recovered by distillation. In this step, alcoholic vapours are stripped from the feed and condensed to produce a first ethanol-rich stream, typically referred to as low wine [71] [70] [9].

2. **Ethanol Concentration:** The low wine stream is fed to the main distillation system, where ethanol is concentrated to approximately 95% by volume [9] [70]. This concentration is achieved through repeated vapour-liquid equilibrium stages in the rectifying section of the column.

3. **Final Rectification and ENA Production:** To achieve **Extra Neutral Alcohol (ENA)**, the 95% ethanol stream undergoes an additional rectification step that raises its purity to values above 96%, consistent with commercial ENA specifications [72]. Aqueous residues from the distillation units (spent lees) are subsequently directed to anaerobic treatment for biogas recovery [9].

4. **By-product Valorization:** The solid fraction of the winery residues, including grape pomace, tartrates, and seeds, is processed separately for the extraction of high-value compounds such as calcium tartrate. Remaining biomass is utilised as fuel in the plant's biomass boiler, contributing to operational self-sufficiency [9] [73].

This integrated process enables the recovery of ethanol from existing winery streams rather than producing it biologically from sugars. It therefore complements conventional winemaking by closing material loops and reducing the environmental footprint of alcohol production.

2.4.2. Case Study: Biorefinería Zambrana

Biorefinería Zambrana, located in the Basque Country (Spain), represents a pioneering national scale implementation of circular bioeconomy principles for the valorisation of wine industry residues. While comparable biorefinery concepts operate in other wine-producing regions worldwide, Zambrana is among the first industrial-scale facilities of its kind in Spain. The plant processes approximately **29,000 tonnes of grape pomace per year**, operating for around **200 days annually in continuous 24-hour shifts**, with production campaigns aligned to the seasonal winemaking period [9].

The biorefinery integrates a multi product portfolio aimed at diverse sectors, including food and beverages, pharmaceuticals, perfumery, animal feed, and energy. From grape pomace, the company recovers a variety of high value compounds such as **bio-ethanol, tartaric acid, polyphenols, seed oil, alcohol free wine, nutritional supplements, and biomass**. This diversification enhances economic resilience while maximizing material recovery [9].

In particular, the production of more than **3 million liters of bioethanol per year** positions the plant as a clear reference point for residue to bioethanol pathways, one of the routes assessed in this study. At the same time, its broader valorization strategy highlights both the opportunities and limitations of current industrial practice compared to emerging alternatives, such as hydrothermal liquefaction (HTL) for biodiesel production. Thus, Biorefinería Zambrana provides not only a commercial benchmark for bioethanol production, but also a practical case against which novel valorization pathways can be critically evaluated in future studies.

2.5. Hydrothermal Liquefaction (HTL) and Upgrading

Hydrothermal liquefaction (HTL) is a thermochemical process that converts lignocellulose biomass (2nd generation) into an energy dense biocrude, along with organics of the aqueous phase, gaseous products and solid residues (typically biochar), under subcritical water conditions, specifically at temperatures ranging from 250 to 374 and pressures between 2-25 MPa [74], [75], [76] [77] [78]. The technique leverages the unique solvent and catalytic properties of high temperature, high pressure water, eliminating the need for extensive feedstock pretreatment[75] [78].

Grape pomace, which consists of skins, seeds, and stems, offers a lignocellulosic feedstock enriched in carbohydrates, lignin, lipids, and bioactive compounds (e.g. polyphenols) [41]. The following sections review the mechanisms of HTL reaction, operational parameters, and valorization pathways, with a specific focus on grape pomace.

2.5.1. HTL Reaction Mechanisms

Under subcritical water conditions, HTL proceeds via four principal stages: hydrolysis, dehydration/decarboxylation, repolymerization, and phase separation [79]. In the context of grape pomace, these reactions are influenced by its high lignin content and various phenolic constituents [79] [41].

1. **Hydrolysis**: Lignocellulosic polymers (cellulose, hemicellulose, lignin) are depolymerized into monomers or oligomers through hydrolysis [79]. For grape pomace, cellulose hydrolysis can be represented as:

   $$(C_6H_{10}O_5)_n + nH_2O \longrightarrow nC_6H_{12}O_6 \tag{2.1}$$

   Hemicellulose decomposes into pentoses (e.g., xylose, arabinose), while lignin undergoes partial depolymerization, releasing phenolic monomers such as guaiacol ($C_7H_8O_2$) [76].

2. **Dehydration and Decarboxylation**: The resulting monomers undergo dehydration ($-H_2O$) and decarboxylation ($-CO_2$), processes that reduce oxygen content and increase the hydrogen to carbon (H:C) ratio [80] [81]. For example, cellulose derived glucose can undergo dehydration to form furans [81]:

   $$C_6H_{12}O_6 \xrightarrow{\text{-H2O}} C_5H_6O_3 \quad \text{(furan formation)} \tag{2.2}$$

   Similarly, acetic acid can undergo decarboxylation to produce methane and carbon dioxide [80] [81]:

   $$CH_3COOH \longrightarrow CH_4 + CO_2 \quad \text{(decarboxylation)} \tag{2.3}$$

3. **Repolymerization**: Reactive intermediates such as phenols, aldehydes, can repolymerize or condense into larger hydrophobic molecules forming biocrude [82] [83]. Maillard reactions, which often occure between carbohydrate derived aldehydes and nitrogenous compounds, contribute to the formation of oil phase constituents [84]:

   $$RCHO + R'NH_2 \longrightarrow RCH{=}N{-}R' + H_2O \tag{2.4}$$

4. **Phase Separation**: Following repolymerization, the products separate into four main phases:

   - **Biocrude (oil phase)**: 30-50 wt% yield, with a higher heating value (HHV) of 30-40 MJ/kg [80] [85] [75].
   - **Aqueous phase**: 15-30 wt%, containing water soluble organics (acetic acid, $C_2H_4O_2$) [80] [85].
   - **Gas phase**: 5-15 wt%, primarily CO_2 with trace CH_4 [80] [85].
   - **Solid residue (char)**: 5-20 wt%, comprising carbonaceous material and inorganic minerals [75], [85].

2.5.2. Operational Parameters

Recent studies have shown that the effectiveness of hydrothermal liquefaction (HTL) is highly dependent on a series of operating parameters, each of which can significantly alter the reaction pathway, product distribution, and overall process efficiency [79]. The main factors that can affect the HTL process are:

Biomass Composition

Grape pomace typically contains cellulose (12- 25%), hemicellulose (5-15%), lignin (15- 30%), lipids (2-8%) and polyphenols (e.g. resveratrol, $C_{14}H_{12}O_3$) [86] [41].

- **Carbohydrates**: A high cellulose content can increase biocrude yields (up to 38 wt %) while also increasing the oxygen content in the oil (~20 wt%) [86].

- **Lipids**: Fatty acids (e.g., oleic acid, $C_{18}H_{34}O_2$) help to increase the Higher heating value (HHV) of biocrude (35-40 MJ/kg) [87].

- **Ash/Inorganics**: Potassium and calcium can enhance char formation (>25 wt%) through crosslinking and catalytic pathways [88].

Moisture Content

HTL operates with liquid water as the reaction medium, making feed moisture a key parameter. For grape pomace, 65-75% moisture is generally optimal [89] [90].

- **Low moisture** (<50%): Insufficient hydrolysis and reduced oil yields [91]
- **High moisture** (>80%): Dilutes reacting intermediates, decreasing overall oil yields [91] [90].

Temperature and Residence Time

Typical HTL operating conditions for biomass fall within a temperature range of 250 to 375 °C, with residence times between 15 and 60 minutes [92].

- **300-320 °C**: Commonly applied for lignocellulosic and agro-industrial residues and associated with efficient depolymerisation and stable biocrude yields [92].
- **330-350 °C**: Higher temperatures promote increased decarboxylation and deoxygenation but may also lead to increased gas formation [85].
- **Residence time**: 15-60 minutes is widely reported as the typical operating window for most feedstocks [92]. Longer durations, extending up to several hours, have been explored for more recalcitrant materials such as sewage sludge.

Pressure and Heating Rate

- **Pressure** (15-20 MPa): Maintains the subcritical density of water (0.7- 0.9 g, cm^{-3}) and supports better heat/mass transfer [77].
- **Heating rate** (>50 $°C\,min^{-1}$): Rapid heating reduces undesirable char formation by limiting prolonged exposure to intermediate temperatures [74] [77].

2.5.3. Equipment Overview

A typical HTL system consists of a high pressure reactor, heating elements, and pressure regulation devices [77] [79]. Batch reactors (autoclaves) are commonly used in research, while continuous systems, which employ high pressure pumps and heat exchangers, are better suited to scale up [79] [77]. Construction materials (e.g., stainless steel, Hastelloy) must withstand corrosion, high temperatures, and pressures for sustained operation [80].

2.5.4. Product Valorization

Biocrude

- Upgrading: HTL biocrude generally requires further upgrading to reduce oxygen, nitrogen, and sulfur content and to improve stability. Common upgrading routes include catalytic hydrodeoxygenation (HDO) using catalysts such as $NiMo/Al_2O_3$, hydrocracking, and hydrotreating, all of which enhance fuel quality and compatibility with refinery infrastructure [76].
- Combustion: HTL biocrudes typically exhibit heating values around 33–36 MJ/kg and can be used in industrial boilers, although viscosity, corrosiveness, and heteroatom content often necessitate pre-treatment or co-firing strategies [76].

Aqueous Phase

- Fertilizer: Contains nitrogen, phosphorus, and potassium (3-5 wt %) [93].
- Anaerobic Digestion: Organic acids and sugars produce 200-300 mL CH_4 /g COD [75].

Solid Residue (Char)

- Soil Amendment: Improves soil water retention and structure [29].
- Activated Carbon: Chemical activation (e.g., KOH) can yield surface areas exceeding 500 m^2/g [86].

Gas Phase

- Energy/Process Integration: CO_2 and CH_4 can be recovered for the generation of heat / power on site or the cultivation of algae [74].

2.6. Biocrude Upgrading to Sustainable Aviation Fuels (SAFs)

The conversion of hydrothermal liquefaction (HTL) biocrude into Sustainable Aviation Fuels (SAFs) represents a pivotal stage in the valorization of wet organic residues into high value hydrocarbons compatible with the aviation sector. The HTL biocrude obtained from feedstocks such as sewage sludge, food waste, or agricultural residues typically contains high concentrations of oxygenated, nitrogenous, and polar compounds, resulting in high viscosity, acidity, and poor thermal stability [64], [94]. Consequently, catalytic upgrading through **hydrogenation** (or hydrotreatment) is recommended to transform the chemically heterogeneous biocrude into hydrocarbon fractions compliant with ASTM D7566 jet fuel standards [95] [96].

Importantly, Sustainable Aviation Fuel (SAF) is considered a drop-in replacement for conventional jet fuel, as its hydrocarbon composition is chemically identical to petroleum derived Jet A-1 kerosene, with the same physical and combustion properties [96]. The only distinction lies in its renewable origin and significantly lower carbon footprint [96]. SAF is therefore fully compatible with existing aircraft engines, fuel handling systems, and is certified under the same specifications [97]. In commercial practice, current aviation standards allow SAF to be blended with conventional jet fuel in proportions of up to 50% by volume, allowing gradual decarbonization of the aviation sector while maintaining full operational safety [96] [97].

Hydrogenation is the fundamental upgrading step in this process, involving the catalytic addition of hydrogen under elevated pressure and temperature to remove heteroatoms and saturate unsaturated bonds [98]. Typical operating conditions range between 300–450 °C and 80–200 bar, employing transition metal sulfide catalysts such as $NiMo/Al_2O_3$ or $CoMo/Al_2O_3$ [95] [98]. During this stage, three key reactions occur: hydrodeoxygenation (HDO), hydrodenitrogenation (HDN), and hydrodesulfurization (HDS), producing water, ammonia, and hydrogen sulfide as by-products [98]. These reactions substantially improve the hydrogen to carbon ratio (H/C), increase heating value, and decrease corrosiveness, thus yielding a more thermally stable hydrocarbon mixture [98].

Following primary hydrogenation, additional refining steps such as **hydroisomerization** and **hydrocracking** are applied to tailor the carbon chain length distribution to the kerosene range (C_8–C_{16}), enhancing cold flow properties and meeting jet fuel boiling range specifications [99] [100]. Hydroisomerization introduces controlled branching to improve fluidity and freeze point, while hydrocracking cleaves heavier paraffinic and naphthenic molecules into lighter, aviation suitable fractions. The resulting mixture predominantly contains normal and iso-paraffins, cycloalkanes, and a minor aromatic fraction—collectively known as synthetic paraffinic kerosene (SPK)—which matches the physical and combustion properties of conventional Jet A-1 fuel [100] [95].

2.6.1. Molecular Composition and Carbon-Chain Distribution in SAFs

The chemical composition of SAFs derived from HTL biocrude closely mirrors that of petroleum based jet fuels, with carbon numbers typically spanning C_7–C_{17} and an average molecular weight centered around C_{11}–C_{12} [100]. According to the U.S. Department of Energy Bioenergy Technologies Office (BETO [100]), conventional jet fuels consist primarily of four hydrocarbon families: n-alkanes, iso-alkanes, cycloalkanes, and aromatics [100]. These species are distributed nearly symmetrically across the jet fuel carbon range (Figure 2.3), with most of the composition arising from molecules containing 9–15 carbon atoms and an average of 12 [100]. Oxygenated compounds, olefins, and heteroatom containing species are either removed or highly restricted due to their adverse effects on freeze point, gum formation, and thermal stability [100].

In SAFs produced from HTL biocrude, the bulk of the hydrocarbon content lies between C_9 and C_{15}, peaking near C_{11}–C_{12}, with n- and iso-alkanes dominating the mixture and cycloalkanes contributing 20–30 wt% [95] [100]. Aromatics, when present, are typically limited to below 25 wt%, consistent with ASTM D1655 and D7566 specifications [100]. This distribution ensures the correct balance between density, volatility, and energy content, providing high combustion efficiency while maintaining a low freezing point (-40 to -47 °C) and suitable flash point (38 °C).

The hydrocarbon family distribution is depicted in Figure 2.3, adapted from the BETO (2020) report [100]. The chart shows the relative weight percentages of n-alkanes, iso-alkanes, cycloalkanes, and aromatics in a representative Jet A fuel (POSF 10325), which serves as a benchmark for SAF molecular design.

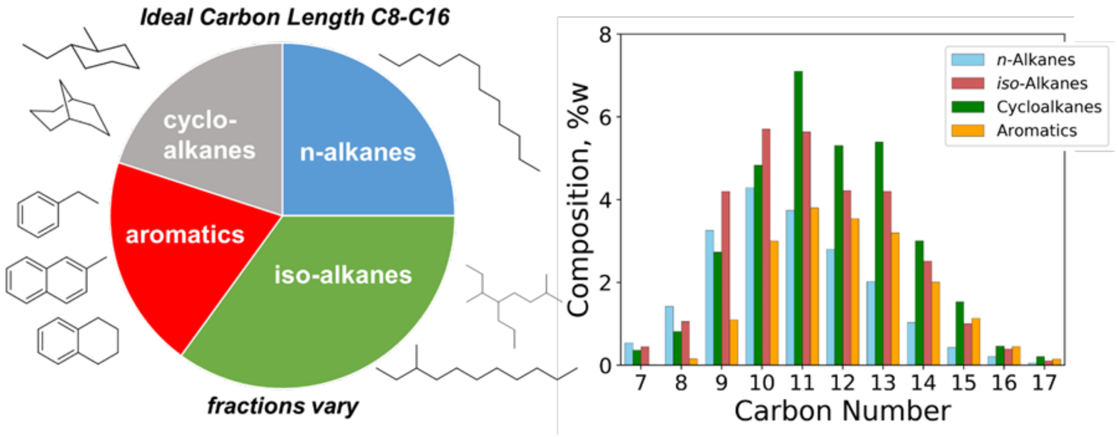

Figure 2.3: Molecular family composition and carbon number distribution of conventional Jet A fuel across the C_7–C_{17} range [100].

Following hydrogenation and hydroisomerization, SAFs produced via the HTL pathway achieve hydrocarbon distributions and physical properties nearly indistinguishable from conventional jet fuel, validating their classification as “drop-in” fuels under ASTM D7566 [96] [100].

Fractional distillation of the upgraded oil is subsequently conducted to recover distinct fuel cuts. The light fraction (C_1–C_4) corresponds to gaseous hydrocarbons, whereas the middle fraction (C_8–C_{16}) constitutes the SAF product stream. Heavy residues may be recycled for further upgrading or tar production [101].
The integration of HTL and catalytic hydrogenation provides a promising pathway to decarbonize aviation fuels. Compared to conventional routes such as Fischer–Tropsch (FT) or Hydroprocessed Esters and Fatty Acids (HEFA), the HTL hydrogenation route offers several advantages: it processes wet feedstocks without drying, achieves high carbon recovery (60–70%), and delivers energy efficiencies of up to 85–90% while utilizing low cost residues [95].

Overall, the hydrogenation of HTL biocrude constitutes a viable and scalable route toward sustainable aviation fuel production, bridging waste management, renewable hydrogen utilization, and the decarbonization of the aviation industry.

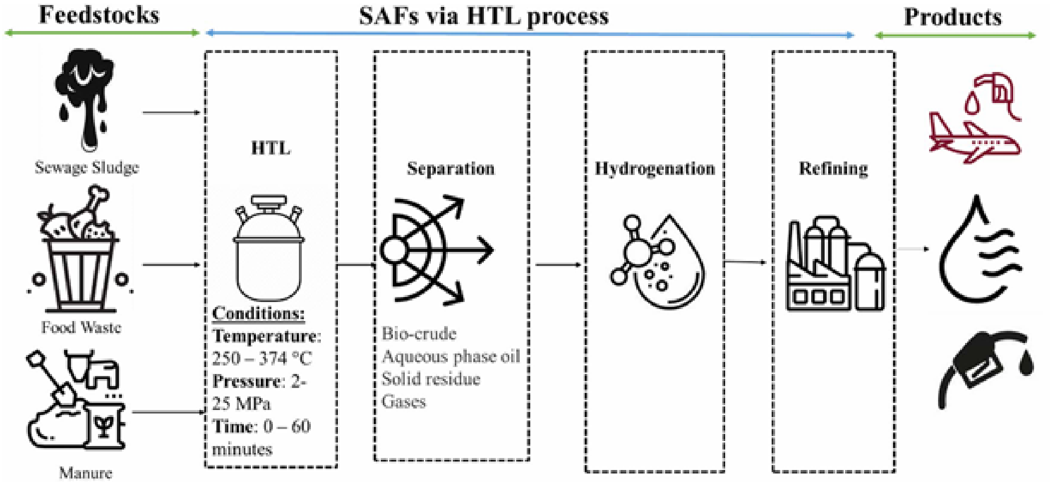

Figure 2.4: Schematic representation of the Sustainable Aviation Fuel (SAF) production route via the Hydrothermal Liquefaction (HTL) process, including feedstock conversion, separation, catalytic hydrogenation, and refining stages. Adapted from [95].

2.6.2. Analytical Characterization of HTL Products

In order to develop an accurate and representative simulation of the upgrading process, a comprehensive characterization of the Hydrothermal Liquefaction (HTL) products is essential. The output of the HTL process, including raw BioCrude, BioChar, the aqueous phase, and gaseous/light organics, must be thoroughly analyzed to determine their chemical and physical properties.

First, the yield percentages will be calculated using the equations provided in the SOP [102]. These equations are as follows:

$$\text{Bio Oil product yield (BOY)} = \frac{W_{biooil}}{W_{dryfeed}} \cdot 100\% \tag{2.5}$$

$$\text{Biochar product yield (BCY)} = \frac{W_{biochar}}{W_{dryfeed}} \cdot 100\% \tag{2.6}$$

$$\text{Aqueous product yield (AY)} = \frac{W_{aqueous}}{W_{dryfeed}} \cdot 100\% \tag{2.7}$$

$$\text{Gas product yield (GY)} = 100\% - BOY - BCY - AY \tag{2.8}$$

Where, W_{biooil} is the weight of bio oil [g],$W_{dryfeed}$ is the weight of feed in dry basis [g], W_{char} is the weight of biochar [g] and $W_{aqueous}$ is the weight of the aqueous phase [g].

With the product yields determined, it is also necessary to characterize the physical and chemical properties of each fraction to develop a realistic simulation of the upgrading process. These characterizations provide essential input parameters for the model and guide decisions on separation and upgrading strategies. Where experimental data cannot be obtained due to limited resources or insufficient sample quantities, representative values will be obtained from the scientific literature to ensure completeness of the analysis. Therefore, the following analytical techniques will be employed:

- **CHN Elemental Analysis**
  This test quantifies the carbon (C), hydrogen (H), and nitrogen (N) content of organic materials. It is essential for determining the empirical formula and energy content of the products [103]. The CHN analysis will be conducted on the Raw BioCrude, BioChar, and the initial biomass feedstock. These measurements are crucial to accuratly model the initial feedstock, evaluate the carbon and nitrogen recovery efficiencies and estimating the higher heating value (HHV) of the products.

- **Proximate Analysis**
  This standard test determines moisture content, volatile matter, fixed carbon, and ash content in solid samples [104]. It will be conducted on the BioChar to evaluate its fuel quality and combustion behavior, as well as its potential for applications such as soil enhancement or activated carbon production [104].

- **Inductively Coupled Plasma Optical Emission Spectroscopy (ICP-OES)**
  ICP-OES enables the detection and quantification of trace metal elements in liquid and solid matrices [105]. This analysis will be applied on the Raw biomass, the BioChar and the aqueous phase. In Raw biomass and BioChar, it identifies the presence of inorganic species or potential catalyst poisons [105]. In the aqueous phase, it assesses the concentration of dissolved metals and nutrients, which is relevant for evaluating the potential for water recycling or environmental discharge [105].

- **Gas Chromatography-Mass Spectrometry (GC-MS)**
  GC-MS is used to identify and quantify volatile and semi volatile organic compounds [106]. This analysis will be conducted on the light organic fraction (e.g., solvents or low boiling fractions recovered during distillation of the BioCrude). Understanding the molecular composition of these fractions is critical for predicting and modelling product behaviour during upgrading [106].

Chapter 3

Pathway 1: Bio-Ethanol Production

This section details the methodology implemented at the Zambrana biorefinery for the valorization of wine industry residues into high-value products, including bioethanol, Extra Neutral Alcohol (ENA), tartrate, biogas, and other co-products. The process is designed to maximize resource recovery, ensure sustainability, and integrate energy efficiency across the production chain. The description in this document follows the process configuration and operational philosophy outlined in the proprietary technical documentation [107]. Although each unit operation is explained in detail in the following subsections, a complete process flow diagram with all unit labels (e.g., Unit 500 – Pomace Stripping, Unit 1500 – ENA Distillation) is also provided in Appendix A for reference.

3.0.1. Feedstock Reception and Pre-treatment

The production process initiates with the collection and storage of red and white grape pomace (Unit 100). The red pomace, obtained post-fermentation, is pressed and stored in reinforced, closed structures to prevent aerobic degradation [9]. White pomace undergoes controlled anaerobic fermentation within storage areas, aided by yeast addition and percolation water recirculation. Both pomace streams are mechanically conveyed for further treatment [9].

3.0.2. Alcohol Recovery and Standardization

In Unit 500, pomace undergoes steam-assisted stripping to extract residual alcohol, which is subsequently concentrated to 92°C GL. The stripped alcohol is directed toward either ENA distillation or bioethanol dehydration, while the solid residue is sent for tartrate recovery or biogas production. Lees are processed in Unit 800 using a single distillation column, generating a compatible alcohol stream and sending spent lees to either tartrate or biogas pathways [9].

3.0.3. Tartrate and Biomass Valorization

Post-stripping, the exhausted pomace is washed with slightly acidic water (Unit 1300) to recover dissolved tartrate. The wash water is evaluated and directed either to tartrate crystallization or wastewater treatment. Pomace is then mechanically pressed (Unit 1600) to reduce moisture before drying and biomass valorization [9].

3.0.4. Ethanol Rectification and Purification

Raw alcohol ranging from 15% to 92% vol is subjected to multi-column distillation in Unit 1500 to achieve ENA quality. The train includes a rectification column, hydroselection column, fusel oil separator, and demethylization column. Thermal integration among the columns reduces steam consumption. Methanol and congeners are separated, and final ethanol purity exceeds 96.2° GL[107].

3.0.5. Drying, Separation and Biogas Generation

Dewatered pomace is dried in rotary dryers (Unit 1700), followed by mechanical separation of seeds and skins. Seeds are stored for oil extraction; peels are reused or valorized. Vapors and particulates generated are treated via cyclones, electrostatic precipitators, and scrubbers (Unit 1800), achieving high emission control efficiency [9].

3.0.6. Bioethanol Dehydration

Unit 1900 dehydrates ethanol using adsorption-reactor trains with zeolite beds. Alternating cycles of adsorption and regeneration ensure near-continuous operation. Regeneration is driven by a vacuum-assisted, heat-integrated system, achieving final ethanol concentrations up to 99.8%[107] [9].

3.0.7. Utility Systems

Utilities play a critical role in process integration [9]:

- The CIP system (Unit 2000) ensures hygienic conditions through optimized cycles of caustic, acid, and water cleaning.

- The biomass boiler (Unit 2200) provides steam at 12 bar, integrating renewable fuels and softened water treatment.

- Cooling towers and chillers (Unit 2300) supply process cooling and safety subcooling for ethanol storage.

- A compressed air system (Unit 2400) supports automation and control valves across the plant.

3.0.8. Wastewater and Byproduct Management

Anaerobic digestion (Unit 2600) treats high-BOD effluents to produce methane-rich biogas, while aerobic treatment (Unit 2700) completes the purification process, ensuring discharge compliance. Calcium tartrate is recovered through acidification, neutralization, precipitation, and drying steps in Unit 2800.

This integrated methodology represents a benchmark for circular bioeconomy applications in the agri-food sector[107].

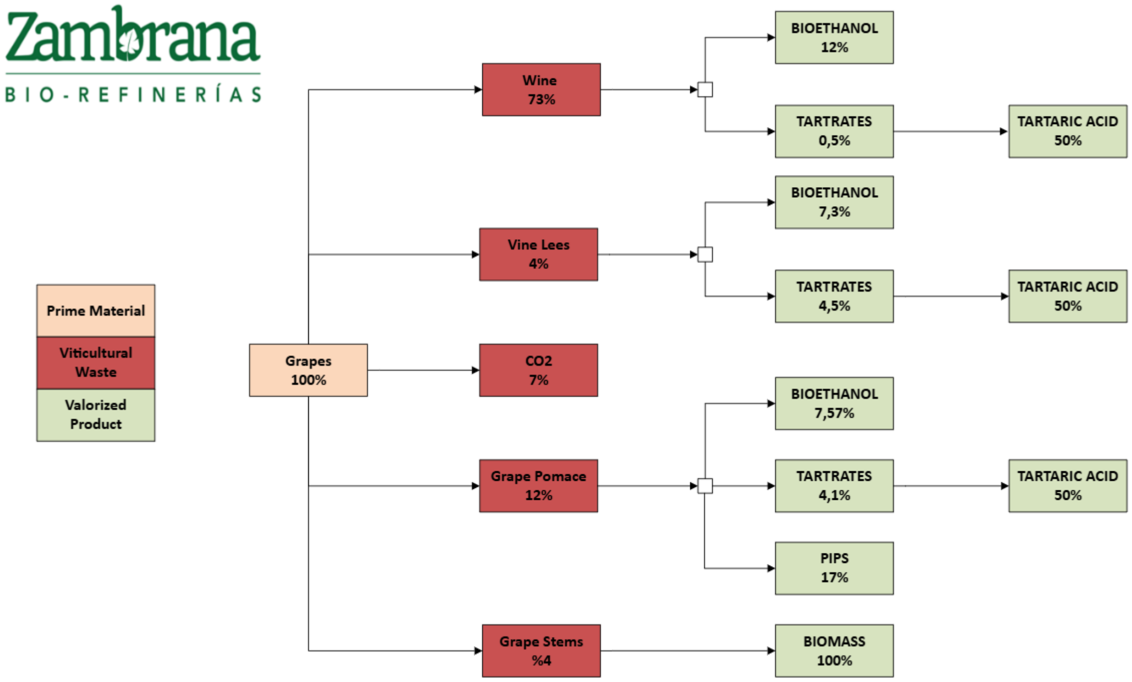

Figure 3.1: Production breakdown at Biorefineria Zambrana [9]

3.1. Economical Analysis

The economic analysis of the bioethanol production pathway has been performed with data provided by Biorefinera Zambrana [9]. This section aims to systematically break down all the cost components and revenue streams associated with the plant. The objective is to assess the financial viability of the project by evaluating key economic indicators, including capital expenditures (CAPEX) and operational expenditures (OPEX).

Capital Expenditure - CAPEX

Capital expenditures (CAPEX) represent the total investment required for the construction and commissioning of the bioethanol production facility. This includes costs associated with equipment procurement, plant infrastructure, construction, installation, and commissioning. A breakdown of these costs can be seen in table 3.1 [9].

Table 3.1: Capital Expenditure cost breakdown for Biorefineria Zambrana [9]

Development Stage	**Cost €**
Land and natural goods	12,313,725
Machinery	19,233,503
Technical Installations	1,389,54
Furniture	1,262
Data Processing Equipment	5,191
Total CAPEX	**32,943,503**

Operational Expenditure -OPEX

This subsection presents the operating expenses (OPEX) of the plant, which include water and power requirements, as well as the consumption of key chemicals essential for the process. Most of the data has been sourced from a feasibility study conducted by Grupo Vento - IN DETEC [108], as part of a proposed process for Biorefinera Zambrana. Additional data was provided by the technical team at Biorefinería Zambrana [9]. It is important to note that labor costs are not included in this analysis, as the second production pathway under consideration operates without dedicated personnel, thereby making direct salary expenditures irrelevant to this comparison. The biomass of the boiler cannot be counted towards the OPEX of the process as the biomass used will come from the unused grape pomace and lees of the winemaking process that reached the biorefinery.

Table 3.2: Updated consumption and operating costs for Biorefinería Zambrana [9]

Consumption	**Quantity (Tn/year)**	**Price (€/Tn)**	**Total Expenditure (€/year)**
Process Water	18,218.2	1.47 [109]	€ 27,780.75
Nitric Acid	721.7	219.3 [110]	€ 158,268.81
Calcium Carbonate	583.7	236.5 [111]	€ 138,045.05
Electricity Consumption (0.117 €/kWh)		Energy kw/h	
Line - Pomace	29,000	870	€ 415,303.20
Line - Lees	6,667	370	€ 51,948.00
Line - Wine	4,000	175	€ 24,570.00
Total Electricity Cost			**€ 491,821.20**
Total OPEX for Services			**€ 815,915.81**

Revenue

Biorefinerías Zambrana operates with a diversified production scheme in which multiple feedstocks and process lines contribute to a range of value added products and by-products. The principal revenue sources stem from the valorization of grape pomace, wine lees, and overproduced wine, as illustrated in Figure 3.2. Notably, a portion of the wine produced by associated wineries is intentionally diverted to the biorefinery as a controlled waste stream. This practice helps maintain the exclusivity of the wineries' commercial portfolio while ensuring a stable feedstock supply for bio based product generation.

In addition to these streams, the facility processes polyphenol rich extracts and non alcoholic wine fractions, further broadening its product portfolio. The integration of these additional lines Grape Pomace (29,000 t/year), Lees (6,667 t/year), Wines (4,000 t/year), Poliphenols (3,600 t/year), and 0,0 Wines (200 t/year) significantly enhances the plant's overall revenue potential.

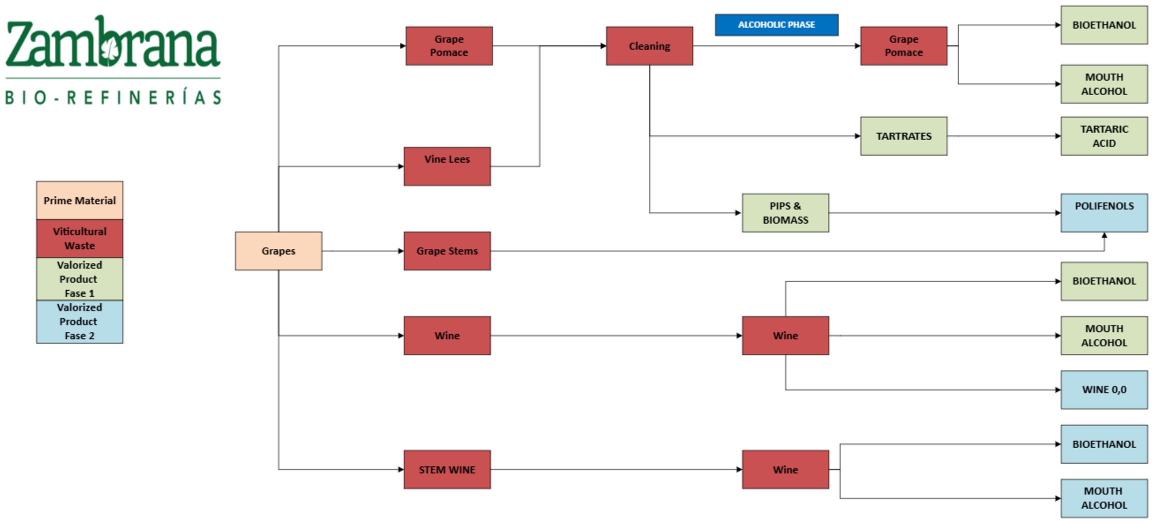

Figure 3.2: Production diagram at Bio-Refineria Zambrana [9]

The revenues generated from the various products are summarized in Table 3.3. The production quantities for each product are based on the plant's expected output after 2030, reflecting the phased operational startup strategy. This approach ensures a realistic assessment of revenue potential once full production capacity is achieved. As shown in Table 3.3, multiple production pathways can yield the same end product. For the purpose of this revenue analysis, the total production volume will be considered, regardless of the specific raw material used in each pathway.

Although Tartrates do appear as a valorized product in 3.3, the main goal for Biorefineria Zambrana is to sell the end product as Tartaric Acid, increasing the profitability of the product

Table 3.3: Yearly Production numbers and revenues [9]

Product	**Quantity**	**Price (€/unit)**	**Total Revenue (€/year)**
Bio-Ethanol	**3,076,857 L**	3.0	9,230,571
Mouth alcohol	**50,000 L**	12.5	625,000
Tartaric Acid	**710,886 L**	5	3,554,430
Wine 0,0	**440,000 L**	3	1,320,000
Pips & Biomass	**5,887,524 kg**	0.1	588,725.40
Poliphenols			
Polyphenol from red skin	**36,000 kg**	50	1,800,000
Polyphenols from white skin	**60,000 kg**	60	3,600,000
Polyphenols from white seeds	**22,000 kg**	40	880,000
anthocyanins	**20,000**	3	66,000
Total Yearly Revenue for Products			**€ 21,664,753.40**

Chapter 4

Pathway 2: Hydrothermal Liquefaction (HTL)

This section outlines the methodological framework adopted to evaluate hydrothermal liquefaction (HTL) as a viable pathway for converting wine industry residues into liquid biofuels. HTL is a thermochemical conversion process that operates under subcritical water conditions (typically 250–375°C and 10–25 MPa), making it particularly suitable for wet biomass such as grape pomace, without requiring prior drying [76] [77].

The methodology follows a sequential and integrated approach that combines literature-based data gathering with process simulation. The characterization of the grape pomace feedstock is based on ultimate and proximate analysis values reported in the literature, which were subsequently normalised to match the mass basis of the feed used in this study. The moisture content was provided directly by Biorefinerías Zambrana [9]. These properties supply the essential input data required for both the conceptual design of the HTL experiments and the configuration of the simulation models.

Following the feedstock characterization, a series of laboratory-scale HTL experiments were performed at TU Delft at three temperatures (300,°C, 320,°C, and 340,°C) in order to determine suitable operating conditions for converting grape pomace into biocrude and biochar. All biochar fractions produced across these experiments underwent elemental (ultimate) analysis at TU Delft. Due to analytical resource limitations, only one representative biocrude sample was subjected to detailed compositional analysis via gas chromatography–mass spectrometry (GC–MS) by an external analytical services provider. These datasets provided the compositional basis required for the subsequent simulation and upgrading stages.
Based on the selected feedstock composition and the experimental outcomes, a comprehensive simulation model was developed in Aspen Plus to represent the HTL process and the subsequent upgrading stages at a conceptual industrial scale. The model incorporates mass and energy balances, yield estimates, and process parameters calibrated using laboratory results and literature data. It includes post-HTL refining operations such as hydrotreatment, distillation, and phase separation, enabling the evaluation of fuel quality, process efficiency, and potential integration with existing refinery infrastructure.

4.1. Experimental process at TU Delft laboratory

The HTL experimental lab work at TU Delft will be carried out utilizing a PARR Reactor 4560. A reactor capable of going to 340 °C with a vessel of total volume of 300ml

Following the users safety manual of the Parr reactors, the first main point of action is to calculate the Maximum allowable water loading (MAWL). This values can be calculated by utilizing the data sheet and equations provided in the Parr Safety operation manual [112]. The main point to take into consideration is that the vessel can never be filled to more than 2/3 of its available space, this is due to possible pressure increases due to the elevated temperatures used [112].

The following data sheet and equation was provided by the Parr safety manual to properly calculate the MAWL [112].

Table 4.1: Liquid volumes and vapor pressures for water in a closed vessel at elevated temperatures [112]

Temperature	**Vapour Pressure (psig)**	**Volume Multiplier (Sp.VT/Sp.V$_{77ř F}$)**	**% Volume Increase**
300	1230	1.40	40
321	1650	1.50	50
349	2350	1.73	73

$$\text{MAWL} = \frac{0.9 \cdot \text{Vessel Volume}}{\text{Volume Multiplier at Max Temperature}} \tag{4.1}$$

With the table 4.1, equation 4.1 and the known vessel volume of 300mL, the following values for the maximum allowable water volume were calculated. For the experiment performed at 340 °C, the value on the par safety guide at 349 was used as all the values were used as an approximation. The results can be found in table 4.2:

Table 4.2: Maximum Allowable Water Level per experiment

Temperature	**MAWL (mL)**
300	192.86
320	180.00
340	156.07

Once the MAWL values were calculated, it was possible to determine both the required biomass feedstock weight and the corresponding amount of water needed to achieve the appropriate slurry composition. Following the guidelines established by Billing et al. [37], a biomass to water ratio of 15% was adopted, as this ratio is commonly cited as optimal for the operation of biomass slurries.

To determine the appropriate feedstock weight for each experimental condition, several constraints were taken into account: the MAWL (Maximum Allowable Working Load) values presented in table 4.2, the safety recommendation from the Parr Safety Manual, which advises filling no more than two thirds of the reactor volume, the 15% biomass concentration limit established by Billing et al. [37], and the solids content of the biomass. According to data provided by AZTI [113], the grape pomace delivered to TU Delft contained approximately 35% solids, a value which was factored into the calculations to accurately determine the amount of dry biomass present in the slurry mixture.

With everything taken into account, the following calculation were performed to determine the ideal ratio of solid biomass to water:

The raw feedstock has a total mass of 60 g, composed of 35% solids.

$$\text{Mass of solids} = 60\,\text{g} \times 0.35 = 21\,\text{g} \tag{4.2}$$

$$\text{Mass of water} = 60\,\text{g} - 21\,\text{g} = 39\,\text{g} \tag{4.3}$$

If we add 80 g of water to the mixture, the total composition becomes:

$$\text{Total solids} = 21\,\text{g} \tag{4.4}$$

$$\text{Total water} = 39\,\text{g} + 80\,\text{g} = 119\,\text{g} \tag{4.5}$$

$$\text{Total mass} = 21\,\text{g} + 119\,\text{g} = 140\,\text{g} \tag{4.6}$$

The final solid to total ratio is calculated as:

$$\text{Solid mass fraction} = \frac{21}{21+39+80} = \frac{21}{140} \approx 0.15 = 15\% \tag{4.7}$$

The initial feedstock weights and added volume of water can be summarised in table 4.3.

Table 4.3: Biomass and water feedstock weight calculations

	300 °C	**320 °C**	**340 °C**
Weight of Grape Pomace (g)	60.0	60.0	60.0
Required Water Volume (mL)	80.0	80.0	80.0

4.2. Experimental Procedure and Separation Protocol

4.2.1. Process Overview

The overall experimental workflow for the hydrothermal liquefaction (HTL) campaign is summarized in Figure 4.1. The process consists of seven sequential stages that include feedstock preparation, reaction, and product separation. Each block in the diagram represents a distinct operation, which is described in the following sections.

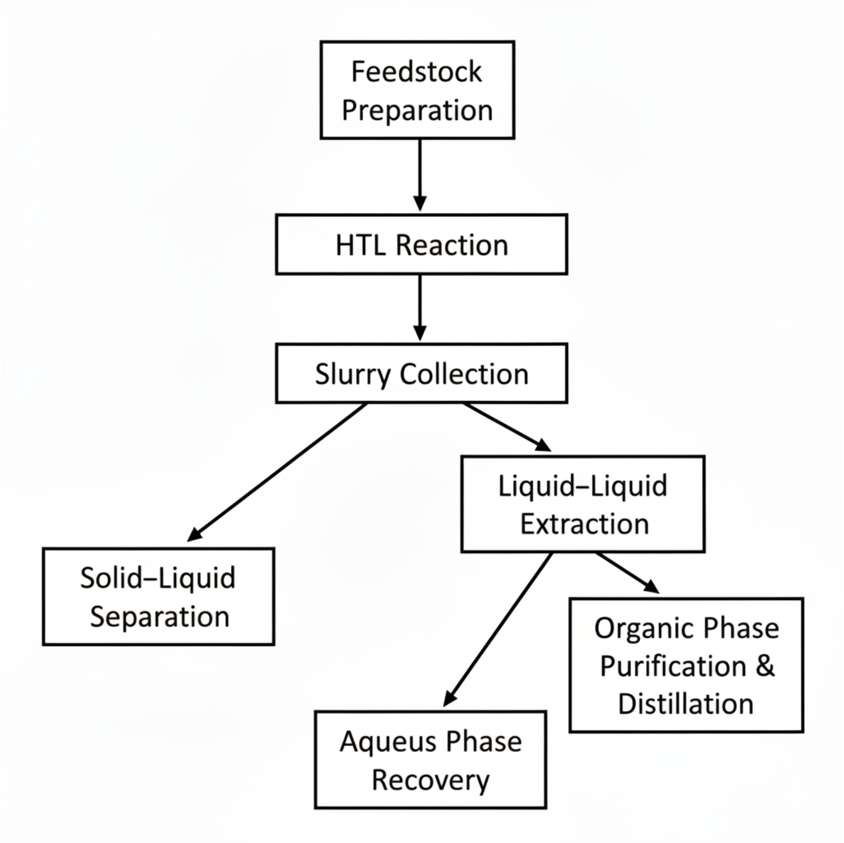

Figure 4.1: Experimental workflow for the HTL process and product separation.

4.2.2. Feedstock Preparation and Reactor Operation

The grape pomace feedstock and demineralized water were weighed to achieve a biomass dry weight of 15 wt%. The mixture was transferred into a 4560 PARR stirred pressure reactor equipped with a mechanical stirrer and thermocouple. After sealing, the system was purged and flushed with nitrogen to establish an inert atmosphere.

The reactor was heated to the target temperature and maintained for a residence time of one hour under continuous stirring. Upon completion, the reactor was rapidly cooled using a circulating cold water bath to quench the reaction. Once the temperature dropped to a safe level, the reactor was disconnected, depressurized, and opened, then the contents were prepared for product separation.

4.2.3. Slurry Collection

After cooling, the entire reactor content; including aqueous liquid, biocrude and solid biochar were carefully collected according to the standard operating procedure (SOP) for HTL product recovery [102]. All internal reactor surfaces (stirrer, thermocouple, and walls) were thoroughly scraped to recover adhering material. The collected mixture was transferred into pre weighed glass beakers for subsequent separation. Approximately 40 mL of dichloromethane (DCM) was used to rinse the reactor interior, ensuring complete recovery of residual organics.

4.2.4. Solid–Liquid Separation

Solid–liquid separation was carried out using a Büchner funnel connected to a vacuum pump. A pre weighed Grade 5 filter paper was placed in the funnel, and the slurry was poured through it. The liquid fraction was collected in a pre weighed flask labeled as the aqueous phase.

After filtration, the DCM rinsate from the reactor was poured onto the remaining solids to extract residual biocrude. Additional rinses of 40–50 mL DCM were applied until the filtrate appeared clear, indicating minimal remaining organics. The retained solids (biochar) were transferred to a petri dish and dried in a convection oven at 105 °C for 12 hours. After drying th sample was weighed to determine biochar yield.

4.2.5. Liquid–Liquid Extraction

The combined DCM filtrates were subjected to phase separation in a 500 mL separatory funnel. An additional 5 mL of DCM was added to facilitate extraction. The funnel was shaken and vented periodically to release pressure, then allowed to rest for phase disengagement. The heavier DCM rich organic phase was drained into a pre weighed round bottom flask, while the lighter aqueous phase was collected separately. A second 5 mL DCM rinse was performed to ensure complete organic recovery.

4.2.6. Aqueous Phase Recovery

The aqueous fraction was recovered using a rotary evaporator (Rotavap) set at 65 °C. Evaporation was carried out gradually under reduced pressure until no visible bubbling occurred, indicating near complete removal of water. The flask was then cooled and weighed to determine the final aqueous yield.

4.2.7. Organic Phase Purification and Fractional Distillation

The DCM rich organic extract was transferred to a pre weighed two neck round bottom flask and subjected to fractional distillation. Initially, low heating power was applied to remove DCM (boiling point 39.6 °C), a process that lasted approximately 30 minutes.

After solvent removal, a second, higher temperature distillation was performed to fractionate the biocrude into light/medium and heavy organic fractions. The heating mantle was increased to reach a steady column temperature of about 328 °C, promoting separation of the more volatile light organics. The mass of the light fraction was recorded as the yield used for subsequent Aspen Plus simulation and upgrading analysis.

4.2.8. Experimental results

A series of HTL experiments were conducted at different temperatures to evaluate how reaction parameters influences product distribution and to identify the conditions that maximise biocrude yield. For each experiment, the biocrude, aqueous phase, gas, and biochar fractions were quantified, and the corresponding yield percentages were calculated on a **dry biomass basis** following the standard procedures outlined in the HTL laboratory SOP [114]. The yield equations used for these calculations are presented in Section 2.6.2, from Equations 2.5 to 2.8. These experimentally derived yields informed the selection of the most representative operating condition and provided the necessary inputs for configuring the subsequent Aspen Plus simulation. The results of the yield compositions for each of the products can be found in figure 4.2.

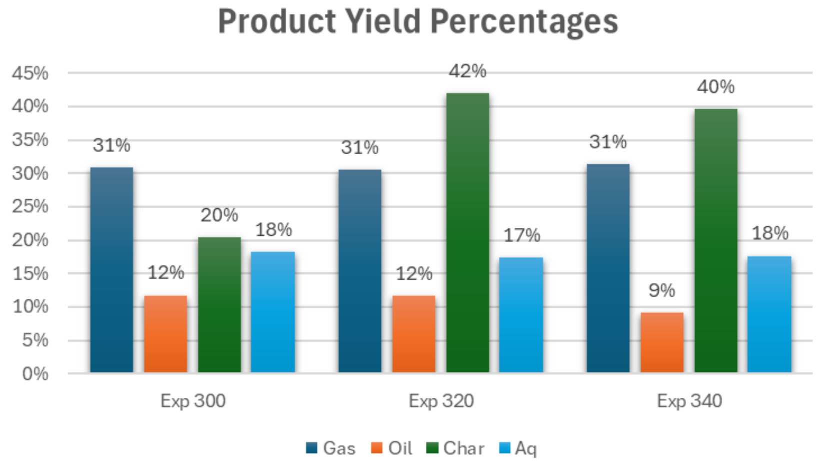

Figure 4.2: Graph of Product yields percentages for each experiment

As it can be observed, there are some discrepancies when observing the common trends of the experiment, specifically regarding the 300 °C experiment. This was due to a malfunction of the drying oven for the biochar, resulting in the filter paper and some of the biochar to combust, reducing the biochar yield by 20%. It was also observed during the experiments that the mass balances were not exactly at 100%, this was probably due to some unevaporated water in the aqueous phase still remaining.

The primary objective was to optimize the process to maximize the bio oil yield (BOY), with a particular focus on maximizing the recovery of the light organic fraction. As shown in figure 4.2, the hydrothermal liquefaction (HTL) experiment conducted at 320 °C achieved the highest yield, reaching 12.22 %. Given the promising outcome at this temperature, the experiment was repeated to verify its reproducibility. The value reported in figure 4.2 represents the average of both test results.

Following the biocrude oil yield obtained, a subsequent distillation was carried out, as described in Section 4.2.7, to fractionate the product into light/intermediate, and heavy organic components. The distillation allowed the recovery of distinct fractions, each quantified as a percentage relative to the initial mass of the biocrude. The distribution of these fractions is presented in figure 4.3.

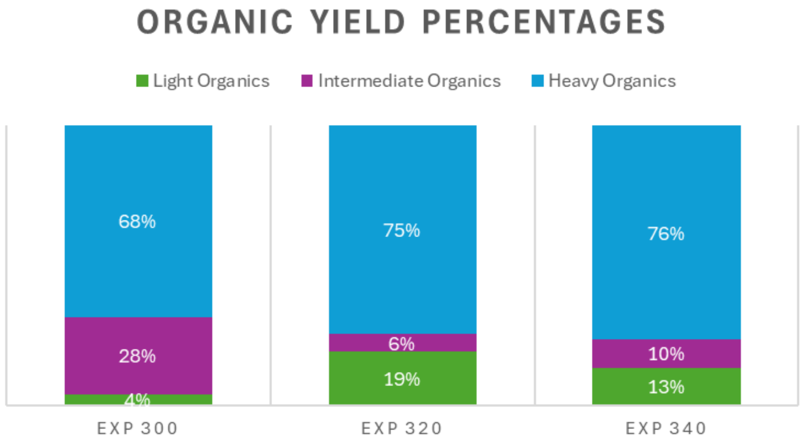

Figure 4.3: Organic fraction yield percentages

To complement the quantitative results, visual documentation of the biocrude fractions obtained from the HTL experiments is provided in Figures 4.4. These images illustrate the physical characteristics and phase distribution of the yields, highlighting differences in color, viscosity, and obtainable quantity.

(a) Raw biomass (b) Biochar (c) Aqueous Phase

(d) Biocrude Oil (e) Heavy Organics (f) Light Organics

Figure 4.4: Raw biomass and the resulting products after Hydrothermal Liquefaction: biochar, aqueous phase, biocrude oil, heavy organics, and light organics.

As mentioned in section 2.6.2, the following laboratory tests were performed on the different yields from the Hydrothermal Liquefaction process. The results can be found in the tables below:

Ultimate (CHNS) Analysis

Ultimate (CHNS) analysis is essential to characterize biomass and hydrothermal liquefaction (HTL) products in terms of elemental composition. These data are required to define nonconventional components in Aspen Plus and to enable subsequent mass and energy balance calculations.

Due to time constraints and technical issues with laboratory equipment, no in house measurements could be performed for the grape pomace feedstock or the HTL biocrude. Therefore, values were adopted from the literature. In contrast, TU Delft measurements were successfully performed for the biochar fraction, allowing for a direct comparison with reported data. The results for each stream are detailed below.

Grape pomace.

The ultimate analysis of grape pomace was taken from Billings et al. [37], who reported the composition of grape residues subjected to HTL. The elemental distribution is summarized in Table 4.4.

Table 4.4: Elemental composition of grape pomace (Billings et al. [37]).

Element	Value [% wt]
Carbon (C)	49.8
Hydrogen (H)	6.1
Nitrogen (N)	1.3
Oxygen (O)*	42.8
Sulfur (S)	0.0

*Oxygen calculated by difference.

Biocrude

For the HTL biocrude, Billings et al. [37] also provide ultimate analysis values, along with a measured higher heating value (HHV). These data were implemented directly in Aspen Plus and are shown in Table 4.5.

Table 4.5: Elemental composition of HTL biocrude (Billings et al. [37]).

Element	Value [% wt]
Carbon (C)	80.3
Hydrogen (H)	9.4
Nitrogen (N)	2.1
Oxygen (O)*	8.2
Sulfur (S)	0.0
HHV (MJ/kg)	38.3

*Oxygen calculated by difference.

Biochar

For the biochar fraction, two data sources were considered. First, Aktaş et al. [115] reported CHNS data for grape pomace biochar obtained from HTL experiments. Second, TU Delft measurements were carried out using a CHNS analyzer on samples produced at 300, 320, and 340 °C. Each condition was analyzed in duplicate, and the values presented here are the mean for each temperature set point.

The 300 °C data were found to be anomalous, with unrealistically low hydrogen values and non physical C/H ratios. As discussed in Section 4.2.8, this was attributed to partial combustion of the material during the drying step. The results are shown in Table 4.6, but the 300 °C values were excluded from the discussion.

Table 4.6: Ultimate analysis of HTL biochar (wt% of analyzed sample).

Metric	Aktaş et al. Aktas2021	TU Delft 300 °C	TU Delft 320 °C	TU Delft 340 °C
C (%)	64.5	53.03	76.24	79.62
H (%)	4.2	0.01	5.54	5.28
N (%)	1.0	4.80	3.17	3.59
S (%)	0.0	0.00	0.34	0.35
C/N (–)	–	11.20	24.04	22.19
C/H (–)	–	$6.2 \times 10^{3\dagger}$	13.89	15.07

*Oxygen and ash were not measured in the TU Delft CHNS runs; by difference oxygen was therefore not reported. [†]The C/H ratio at 300 °C is non physical due to the near zero hydrogen content and is not considered reliable.

The TU Delft measurements at 320 and 340 °C showed higher carbon and nitrogen contents compared to Aktaş et al., consistent with differences in feedstock, operating conditions, or analysis method.

Proximate Analysis

In addition to the ultimate (CHNS) analysis, a proximate analysis was required to characterize the physical and thermal properties of the grape pomace feedstock. Proximate analysis reports the relative fractions of moisture, volatile matter, fixed carbon, and ash, thereby complementing the elemental data by describing the fuel's combustion behavior and inorganic content. These values are also necessary for defining nonconventional solids in Aspen Plus.

Due to time and equipment limitations at TU Delft, no proximate analyses could be performed experimentally. Instead, representative values for grape pomace were obtained from Mazhkoo et al. [116], who reported biomass proximate analyses with a moisture content of approximately 62.14%.

However, based on information provided by the supplier of the grape pomace used in this study, the actual moisture content of the received material was approximately 65% [113]. To ensure consistency with the experimental feedstock conditions, the proximate data reported by Mazhkoo et al. were normalized to this moisture basis. The adjusted composition maintains the same dry basis distribution of volatile matter, fixed carbon, and ash, while accounting for the slightly higher water content in the as received material. The original and moisture adjusted values are presented in Table 4.7.

Table 4.7: Proximate analysis of grape pomace: original data from Mazhkoo et al. [116] and normalized values at 65% moisture.

Property	**Mazhkoo et al. [% wt]**	**Adjusted (65% moisture) [% wt]**
Moisture	62.14	65.00
Volatile Matter	74.50	74.5
Fixed Carbon	19.47	19.47
Ash	6.03	6.03

The high moisture content highlights the need to account for water as a major constituent of the feed stream, consistent with the preparation of the slurry described in Section 5.1.1. The relatively large volatile matter fraction reflects the organic degradability of grape pomace, while the fixed carbon and ash contents represent the non volatile fraction expected to remain in the biochar.

Inductive Coupled Plasma Optical Emission Spectroscopy (ICP-OES)

As explained in Section 2.6.2, ICP–OES analyses were performed to quantify the inorganic elemental composition of selected HTL fractions, namely the raw biomass, solid char, and aqueous phases. This characterization enables the identification of key elements in the process streams and supports the material assessment of the HTL products. Figure 4.5 presents a summary of the elemental composition of the raw biomass and the biochar samples produced at the three reaction temperatures, while Figure 4.6 summarizes the ICP–OES results for the aqueous fraction. A complete breakdown of the elemental concentrations for all samples is provided in Appendix B.

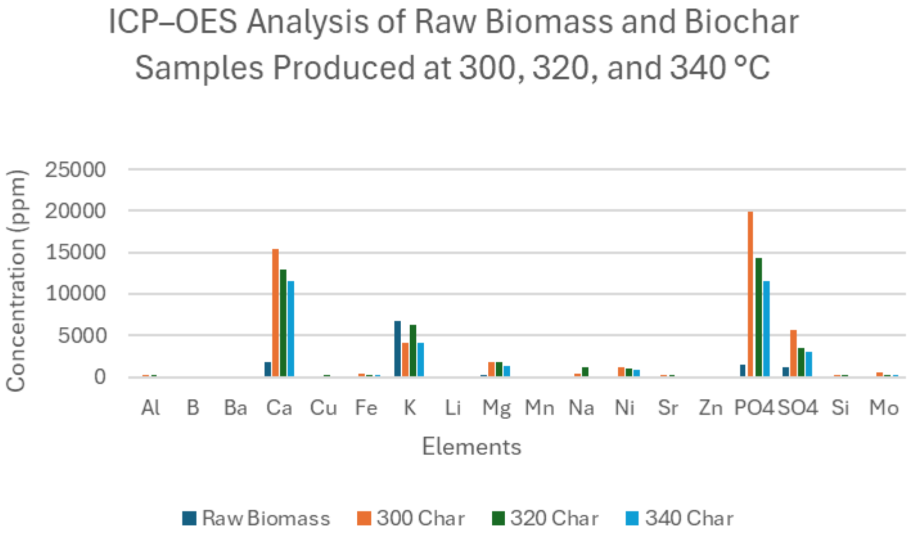

Figure 4.5: ICP-OES analysis results for raw biomass and biochar fractions obtained from HTL experiments

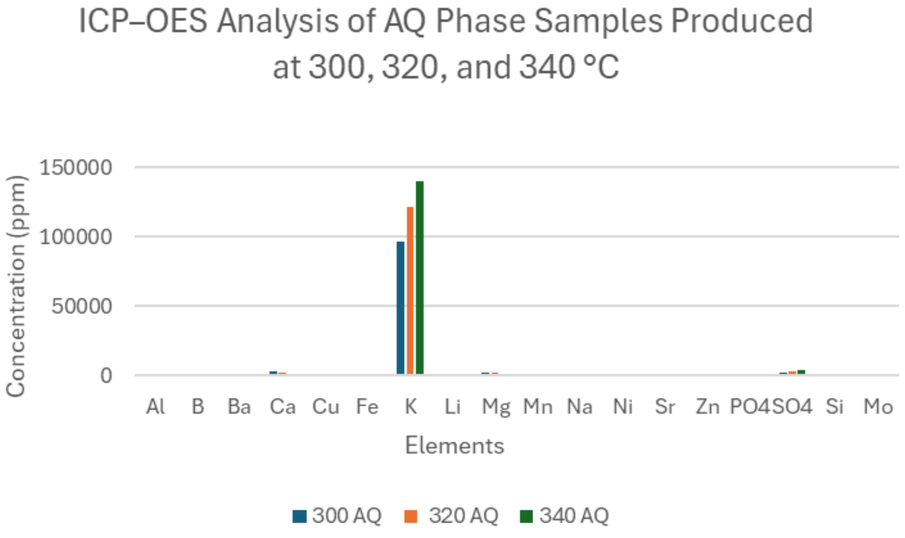

Figure 4.6: ICP-OES analysis results for AQ fractions obtained from HTL experiments

Although the elemental analysis via ICP-OES is not directly critical to the primary objective of this study, it provides valuable insight into the distribution of inorganic elements across HTL by-products. In particular, elements such as potassium (K), calcium (Ca), and magnesium (Mg) were found to be significantly higher in the aqueous phase, while transition metals and phosphorus species (PO_4) were largely retained in the char. This differentiation is particularly relevant for the future valorization of by-products: aqueous streams may serve as nutrient rich fertilizers, while the metal rich char could find applications in catalysis, material recovery, or soil amendment. Thus, while not central to this investigation, the data establish a foundation for a more holistic biorefinery approach to the circularity of grape pomace.

A summary of the normalized distribution of elements in the HTL byproducts for the 320 °C experiment and the raw biomass can be seen in figure 4.7.

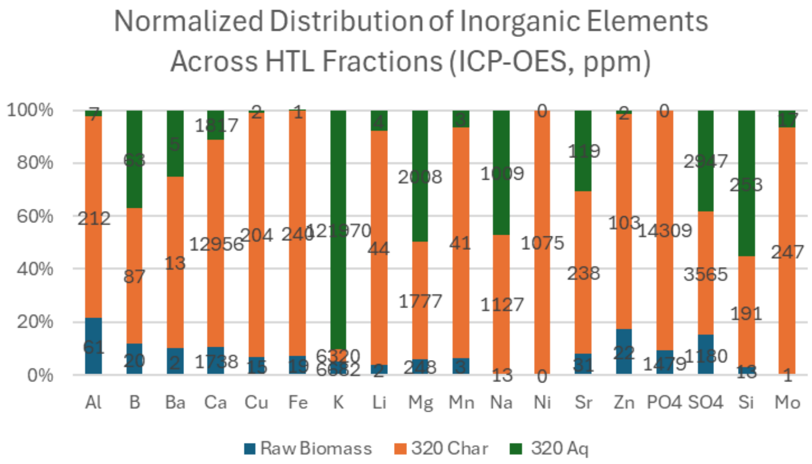

Figure 4.7: Normalized Distribution of Inorganic Elements Across HTL Fractions for the 320 °C experiment and raw biomass (ICP-OES, ppm)

Gas Chromatography-Mass Spectrometry (GC-MS)

The GC-MS analysis of the HTL biocrude light organics revealed a complex mixture of alcohols, ketones, phenolics, aromatics, and long chain hydrocarbons. Figure 4.8 shows the relative area percentages of the most prominent compounds, while the complete compound list is provided in **Appendix C.1**. The most abundant species fall in the 4-6% range, dominated by nitrogenous aromatics, phenolics, and oxygenated cyclopentenones [117][118]. These compounds are characteristic of lignocellulosic hydrothermal liquefaction oils, reflecting partial depolymerization of lignin and cellulose structures [118].

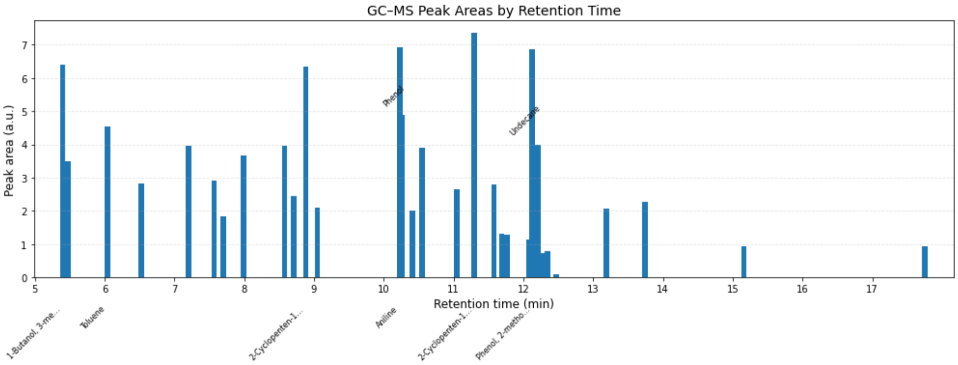

Figure 4.8: GC-MS components and relative area percentages for HTL biocrude Light Organics.

Table 4.8 summarizes the major compounds identified in the HTL biocrude with match qualities above 85% and relative peak areas exceeding 5%. The most abundant component was **2-Cyclopenten-1-one, 2,3-dimethyl- (7.4%)**, followed by **Aniline (6.9%)**, **Phenol, 2-methoxy- (6.9%)**, **1-Butanol, 3-methyl- (6.4%)**, and **2-Cyclopenten-1-one, 2-methyl- (6.3%)**.

Table 4.8: Most abundant GC-MS compounds in HTL biocrude with quality 85% and area 5%.

Compound	**Retention Time (min)**	**Normalized Area (%)**
2-Cyclopenten-1-one, 2,3-dimethyl-	11.2969	7.4%
Aniline	10.2282	6.9%
Phenol, 2-methoxy-	12.1304	6.9%
1-Butanol, 3-methyl-	5.3981	6.4%
2-Cyclopenten-1-one, 2-methyl-	8.8821	6.3%

The complete list of GC–MS identified compounds, including retention times, area percentages, and match quality, is presented in **Appendix C.1**.

Chapter 5

Pathway 2: HTL Simulation + Upgrading via Aspen-Plus

5.1. HTL Simulation, Upgrading and Analysis

Process Scalability Considerations

Although the HTL simulation is grounded in laboratory-scale data obtained at TU Delft, its ultimate purpose is to extrapolate the process to a conceptual industrial scale. This approach enables a consistent comparison with larger systems, including the biorefinery operations examined in the Zambrana case study. While the input masses, temperatures, and yields reflect laboratory measurements, the simulation framework is constructed so that these parameters can be readily adapted to continuous industrial-flow conditions. All downstream process blocks and mass and energy balances preserve the experimentally derived yield fractions and phase behavior, ensuring coherence with laboratory observations while enabling a realistic techno-economic assessment at scale.

5.1.1. Feed Characterization

The grape pomace input was modeled in Aspen Plus as a **non-conventional solid component** to reflect its varied, lignocellulosic nature. Since there was no experimental data on the specific residue during the simulation, we used representative values from existing literature. The ultimate analysis, which includes carbon, hydrogen, nitrogen, sulfur, and oxygen, came from Billings et al [37]. The proximate analysis, covering moisture, volatile matter, fixed carbon, and ash, was calculated and normalized from Mazhkoo et al [116]. These properties defined the elemental and physical characteristics needed for the thermodynamic calculations of the biomass fraction.

To establish the input mass flows, the total annual feedstock supply was set at 29 000 t of wet grape pomace, assuming 200 days of continuous operation per year at 24 h/day. This corresponds to an effective operating time of:

$$t_{\mathrm{op}} = 200 \times 24 = 4800\,\mathrm{h/year}.$$

The average feed rate is therefore:

$$\dot{m}_{\mathrm{wet}} = \frac{29000 \times 10^3}{4800} \approx 6042\,\mathrm{kg/h}.$$

Assuming a dry solid content of 35 %, the corresponding mass flows are:

$$\dot{m}_{\mathrm{dry}} = 0.35 \times \dot{m}_{\mathrm{wet}} \approx 2114.7\,\mathrm{kg/h},$$

$$\dot{m}_{\mathrm{water}} = 0.65 \times \dot{m}_{\mathrm{wet}} \approx 3927.3\,\mathrm{kg/h}.$$

These values were used to define the base feed streams in Aspen Plus, with the water modeled as a conventional component and grape pomace as a nonconventional solid with the proximate and ultimate analyses described above.

To reproduce the solid to liquid ratios applied in laboratory scale hydrothermal liquefaction (HTL) experiments, an additional amount of process water was included in the slurry preparation. This ensured a final feed composition equivalent to 15 % solids and 85 % liquid.

Based on the annual plant throughput of 29.000 t of grape pomace (corresponding to 6.042 $\mathrm{kg\,h^{-1}}$ of wet feed), and considering its inherent moisture content of 65 %, the feed stream consists of approximately 2114.7 $\mathrm{kg\,h^{-1}}$ of dry solids and 3927.3 $\mathrm{kg\,h^{-1}}$ of water.

The amount of additional water W_{extra} required to dilute the feed to the target composition was obtained by solving the following.

$$\frac{m_{\text{solids}}}{m_{\text{solids}} + m_{\text{water,initial}} + W_{\text{extra}}} = 0.15 \tag{5.1}$$

where $m_{\text{solids}} = 2114.7\,\text{kg}\,\text{h}^{-1}$ and $m_{\text{water,initial}} = 3927.3\,\text{kg}\,\text{h}^{-1}$. Rearranging gives:

$$W_{\text{extra}} = \frac{m_{\text{solids}}}{0.15} - (m_{\text{solids}} + m_{\text{water,initial}}) \tag{5.2}$$

$$W_{\text{extra}} = 8056\,\text{kg}\,\text{h}^{-1} \tag{5.3}$$

This adjustment was implemented in Aspen Plus through a `MIXER` block, yielding a final HTL slurry stream of approximately $14\,098\,\text{kg}\,\text{h}^{-1}$, composed of $2288\,\text{kg}\,\text{h}^{-1}$ solids and $12\,962\,\text{kg}\,\text{h}^{-1}$ water. Table 5.1 Provides a breakdown of the composition of the input streams of the simulation.

Table 5.1: Mass flow rates of input streams for HTL slurry preparation

Stream component	**Mass flow (kg/h)**
Dry solids (from grape pomace)	2114.7
Inherent water (in grape pomace)	3927.3
Additional process water	8056
Total HTL slurry	14 098

5.2. Aspen Simulation

The overall Aspen Plus simulation of the hydrothermal liquefaction (HTL) and upgrading process is illustrated in Figure 5.1. The process has been divided into four main sections to facilitate systematic analysis: (i) the HTL reactor, representing the conversion of grape pomace into a multiphase product stream; (ii) the phase separation sequence, where gaseous, aqueous, biochar, and biocrude phases are isolated; (iii) the decomposition and hydrogenation units, responsible for biocrude upgrading through hydrotreatment; and (iv) the final distillation system, which recovers the jet fuel range hydrocarbons from the upgraded liquid product.

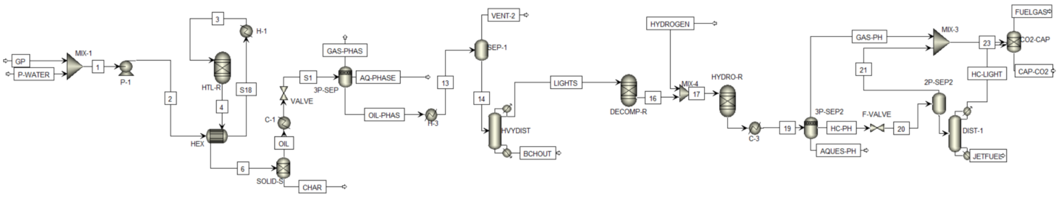

Figure 5.1: Complete Aspen Simulation: Grape pomace to Jetfuel

5.2.1. HTL Reactor Setup

The hydrothermal liquefaction (HTL) process was modeled in Aspen Plus using the flowsheet shown in Figure 5.2. Grape pomace (`GP`) and process water (`P-WATER`) were first combined in a `MIXER` block (`MIX-1`) to form a homogeneous slurry. This mixture was then pressurized to 20 MPa using a `PUMP` (`P-1`), ensuring proper flow conditions throughout the feed section.

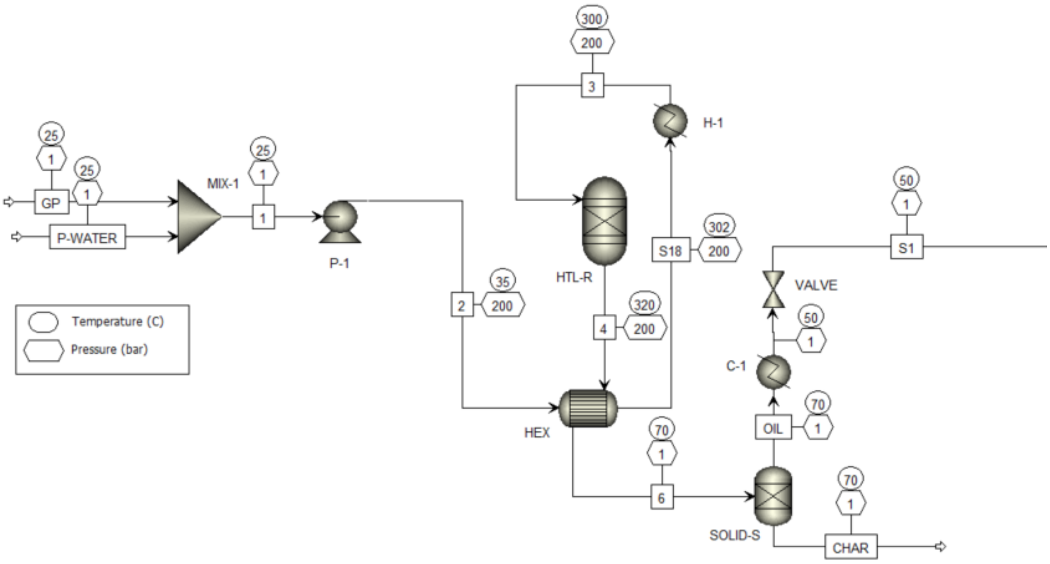

Figure 5.2: Aspen Plus process flowsheet for the updated hydrothermal liquefaction system, incorporating internal heat recovery and solid–liquid separation.

A countercurrent `HEAT EXCHANGER` (`HEX`) was included to enhance the energy efficiency of the process by recovering heat from the reactor effluent. In this configuration, the hot product stream leaving the reactor transfers its sensible heat to the incoming feed prior to entering the heating section. The outgoing stream cools from approximately 320 °C to 70 °C, while the incoming grape pomace slurry is simultaneously preheated from ambient temperature to 175.8 °C. This internal heat recovery significantly decreases the external energy demand of the preheating stage.

After preheating, the slurry is raised to 300 °C in the `HEATER` block (`H-1`), slightly below the target reaction temperature to prevent premature thermal conversion within the heating section. The conditioned feed is then introduced into the `HTL-R` reactor, modeled as a `RYield` block operating at 320 °C and 200 bars. The yield distribution implemented in the reactor reproduces the product fractions obtained experimentally at TU Delft under equivalent operating conditions, as illustrated in Figure 5.3.

The reactor effluent, still at high temperature and pressure, passes through the same `HEX` to release its thermal energy to the incoming stream. The cooled stream (approximately 70 °C) then enters a `SOLID SEPARATOR` (`SOLID-S`), where solid biochar is removed from the aqueous–organic liquid phase.

A total of 14271.29 kg/hr of slurry enters the separator, yielding 927.63 kg/hr of solid biochar and 13343.66 kg/hr containing the biocrude and aqueous fractions. The liquid phase is subsequently cooled to 50°C in a `COOLER` (`C-1`). The stream then passes through a valve to produce a pressure drop from 20 bars to 1 bar.

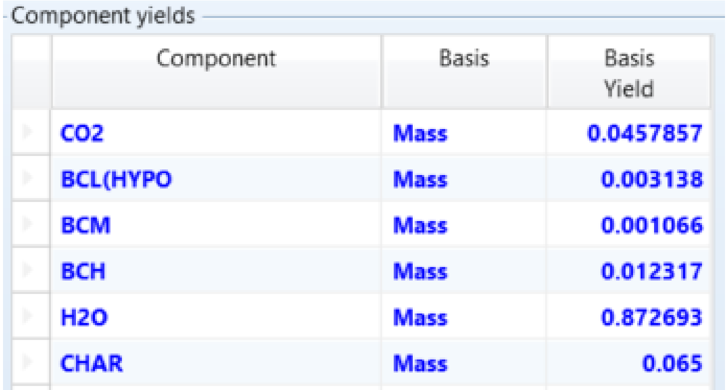
Component yields

Component	Basis	Basis Yield
CO2	Mass	0.0457857
BCL(HYPO	Mass	0.003138
BCM	Mass	0.001066
BCH	Mass	0.012317
H2O	Mass	0.872693
CHAR	Mass	0.065

Figure 5.3: Component yield distribution applied in Aspen Plus for the HTL reactor at 320 °C.

The resulting product slate included gaseous CO_2, water, solid biochar, and three liquid biocrude pseudocomponents:

- **BCL** – biocrude light
- **BCM** – biocrude medium
- **BCH** – biocrude heavy

Reactor modeling approach
The `HTL-R` block was implemented as a `RYield` reactor, in which the nonconventional grape pomace feed is decomposed into a predefined set of conventional components based on experimentally determined yields as shown in figure 5.3. This modeling strategy allows the direct use of laboratory mass balances while avoiding the need to specify detailed reaction kinetics, which are typically unknown or highly complex for biomass liquefaction systems.

The yield distribution was derived from experimental data obtained under identical operating conditions (320°C and 20 MPa). The implemented mass fractions reproduce the experimentally observed distribution between biochar, aqueous phase, biocrude, and gaseous CO_2. However, since the experimental yields were reported on a dry feed basis, normalization was required to express the product distribution relative to the total wet feed entering the reactor. In the experimental setup, the solid fraction represented approximately 15% of the total mass (the remaining 85% corresponding to the intrinsic and added water); therefore, each yield associated with the dry solids was scaled by this factor to ensure mass consistency within the simulation.

Modeling assumptions (RYield setup)
To keep the simulation tractable while maintaining fidelity to the experimental observations at 320 °C and 20 MPa, the following simplifying assumptions were applied in the `RYield` configuration:

1. **Gas phase composition.** The gaseous product was modeled entirely as CO_2. Minor gases such as CO, H_2, or CH_4, usually present in trace amounts, were not quantified in the experimental campaign and therefore omitted without significant impact on the overall mass or energy balance.
2. **Aqueous phase composition.** The aqueous product was represented as pure H_2O. Although water soluble organics (e.g., short chain acids, alcohols, phenolics) are known to form during HTL, they were excluded from the current process scope since no recovery or valorization steps are modelled downstream. This simplification preserves the correct energy balance while avoiding excessive compositional complexity.
3. **Oil phase representation.** The biocrude was lumped into three volatility based pseudocomponents **BCL** (light), **BCM** (medium), and **BCH** (heavy) representing the light distillate, medium distillate and heavy oil fractions, respectively. This lumped approach provides a robust framework for downstream separation and upgrading without requiring detailed compound level speciation. The surrogate physical properties (normal boiling point and density) assigned to these components are described in Section 5.2.2.

These assumptions reproduce the experimentally observed yield distribution while supporting downstream energy integration and separation modeling. Since neither gaseous nor aqueous products are utilized in this study, the simplifications introduce negligible error in the mass and energy balances,

5.2.2. Definition of pseudocomponents

The three biocrude fractions were defined as conventional pseudocomponents in Aspen Plus, with physical properties assigned to reflect their volatility and density characteristics [119]. The normal boiling point (NBP) and density were selected as primary surrogate parameters, as summarized in Table 5.2.

Table 5.2: Pseudocomponent properties defined for HTL biocrude fractions.

Component	**Normal Boiling Point [°C]**	**Density (g/ml)**
BCL (light)	327	785
BCM (medium)	344	789
BCH (heavy)	402	801

For the light biocrude fraction (BCL), individual compound boiling points obtained from the GC–MS analysis were examined. The compound exhibiting the highest boiling point within this fraction, N-benzyl-2-phenethylamine, with a boiling point of approximately 328 °C, was selected as the representative pseudo-component. For the medium biocrude fraction (BCM), a normal hydrocarbon in the C20 range was chosen to represent the typical diesel range compounds, corresponding to a boiling point of approximately 344 °C. Finally, the heavy biocrude fraction (BCH) was characterized by a representative C25 hydrocarbon , reflecting the higher molecular weight paraffinic content and assigned a boiling point of 402 °C.

Biochar definition
The solid biochar fraction was modeled as a nonconventional component in Aspen Plus. Its elemental composition was defined according to the TU Delft CHN(S) analysis of the biochar produced at TUDELFT and the proximate values found in literature, as reported in Table 4.6.

Thermodynamic model
The **NRTL (Non Random Two Liquid)** model was employed as the global thermodynamic framework for the HTL system. This choice is justified by the highly non ideal and polar nature of the aqueous–organic mixtures produced during liquefaction. NRTL provides reliable predictions for both vapor–liquid and liquid–liquid equilibria in mixed polar–nonpolar systems and has been widely applied in biomass liquefaction and biocrude upgrading simulations.

5.3. Phase separation

The cooled HTL product stream was subjected to a sequence of separation steps designed to isolate the gas, aqueous, and oil phases. The overall flowsheet implemented in Aspen Plus is presented in Figure 5.4. This configuration represents a simplified industrial separation train, consistent with the project scope in which only the oil fraction is valorized, while the aqueous and gaseous products are removed from the system.

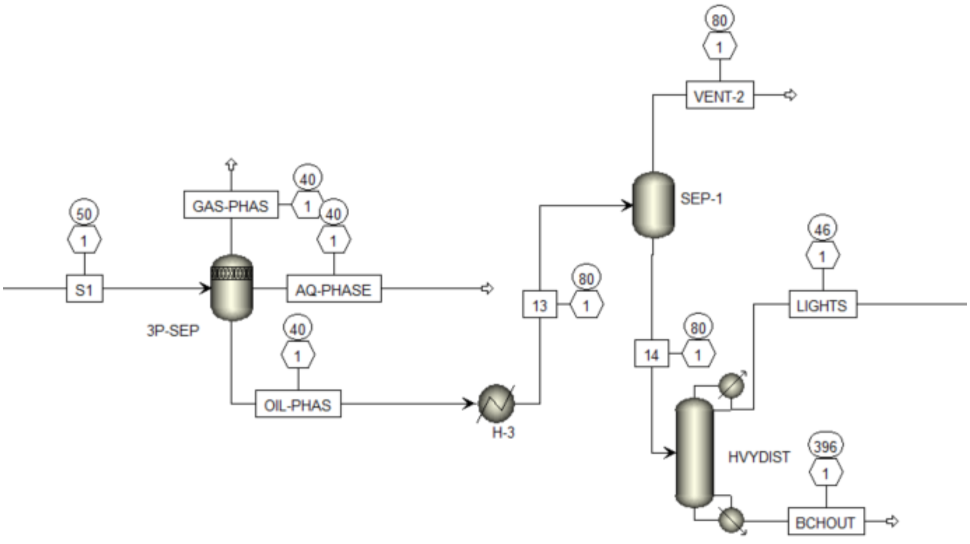

Figure 5.4: Aspen Plus flowsheet for the HTL phase separation and biocrude distillation section.

After cooling to 50 °C, the HTL output stream entered a three phase separator (`3P-SEP`) operating at 40 °C and 1 bar. This unit produced three outlet streams: `GAS-PHAS`, `AQ-PHAS`, and `OIL-PHAS`. The gas phase consisted primarily of CO_2, with trace quantities of light organics; the aqueous phase was composed almost entirely of H_2O, in line with the modeling assumptions described in Section 5.2.1. Both streams were PURGED from the system, as no recovery or valorization steps were included within the present process boundaries.

The `OIL-PHAS` stream, containing the biocrude and minor residual water, was subsequently directed to a `HEATER` (`H-3`) where the temperature was raised to 80 °C. This step served to remove remaining moisture and dissolved CO_2, ensuring that the feed entering the next stage had the least amount of impurities.

The conditioned oil stream was then routed to a separator (`SEP-1`) that allowed venting of trace amounts of H20 vapour and CO2 gase through the `VENT-2` outlet. The liquid effluent was introduced into a distillation column (`HVYDIST`) for removal of the heaviest organic cut (BCH). This column fractionated the biocrude into two streams: a light distillate (`LIGHTS`) and a heavy residue (`BCH`).

This configuration therefore provided a streamlined representation of the liquid phase separation and stabilization sequence following HTL. The light and medium distillate fraction (`LIGHTS`) was selected as the feedstock for subsequent upgrading, while the aqueous, gaseous, and heavy purge streams were excluded from further consideration.

5.4. Decomposition and Hydrogenation of Light Fraction

Following removal of the heavy BCH fraction in the distillation column, the light and medium biocrude stream (`LIGHTS`) was directed to a decomposition reactor (`DECOMP-R`) to convert the pseudocomponents defined in the previous stages into real compounds representative of the experimental biocrude composition obtained through the GC-MS test (AppendixC.1). The overall configuration of this section is shown in Figure 5.5.

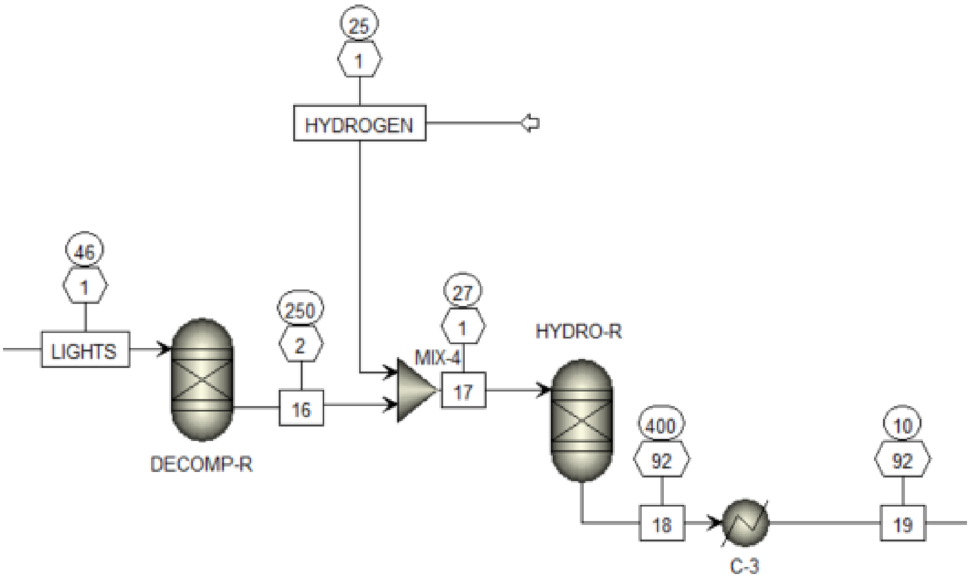

Figure 5.5: Aspen Plus flowsheet for the decomposition and hydrogenation setup.

The main objective of the `DECOMP-R` unit is to replace the lumped pseudocomponents (BCL and BCM) with a realistic distribution of identified molecular species derived from the GC–MS analysis of the HTL biocrude (Appendix C.1). This step enables the transition from generalized surrogate modeling to component specific modelling.

The yield distribution implemented in the decomposer was based on the GC–MS quantification of the light and medium fractions of the biocrude. The relative abundance of each compound was calculated by normalizing its GC–MS peak area to the total detected area and multiplying by the overall mass yield of the light and medium HTL fractions (25%). The resulting composition of the decomposed stream is summarized in Table 5.3.

Table 5.3: Product composition defined in the Aspen Plus `DECOMP-R` reactor (mass fractions).

Component	**Yield** [-]	**Component**	**Yield** [-]
3-MET-01	0.0508	2:4-D-01	0.0314
2-MET-01	0.0278	N-DEC-01	0.0309
TOLUENE	0.0359	3-MET-03	0.0387
CYCLO-01	0.0224	1-MET-01	0.0184
PYRAZ-01	0.0314	CYCLO-04	0.0584
2-MET-02	0.0231	BICYC-01	0.0176
3-MET-02	0.0145	N-BUT-01	0.0222
ETHYL-01	0.0291	C8H12-01	0.0209
STYRE-01	0.0314	METHY-01	0.0103
CYCLO-02	0.0150	O-TOL-01	0.0119
N-NON-01	0.0195	1-UND-01	0.0092
2-CYC-01	0.0503	GUAIA-01	0.0545
2:5-D-01	0.0263	N-UND-01	0.0317
2-MET-03	0.0167	5-UND-01	0.0058
CYCLO-03	0.0413	2-CYC-02	0.0062
ETHENE	0.0291	2-MET-04	0.0007
PHENE-01	0.0388	2:5-D-02	0.0135
ANILI-01	0.0549	N-PEN-01	0.0164
PHENO-01	0.0388	N-DOD-01	0.0181
1-DEC-01	0.0159	N-TRI-01	0.0075
		N-PEN-02	0.0074
H_2O	0.0035	CO_2	0.0023

The decomposed liquid stream exiting the `DECOMP-R` unit was subsequently mixed with a hydrogen feed in the `MIX-4` block to define the inlet composition for the hydrogenation stage. In this configuration, a continuous flow of 700 kg/hr of hydrogen gas was introduced to the decomposed biocrude stream. This value was selected as a representative operating point, ensuring numerical stability and convergence within the simulation while maintaining realistic hydrogen to oil ratios. Lower hydrogen flow rates resulted in convergence issues due to mass balance inconsistencies, whereas higher values had negligible influence on the system's thermodynamic initialization. The selected flow rate therefore provides a stable and physically plausible basis for subsequent upgrading and deoxygenation modeling.

5.4.1. Hydrogenation Reactor and Product Distribution

The hydrogen enriched stream exiting the `MIX-4` block was subsequently directed to the hydrogenation reactor (`HYDRO-R`), where the stabilization and upgrading of the decomposed biocrude took place. The reactor was operated at 400 °C and 92 bar, representative of typical hydrotreating conditions, enabling both hydrogenation and hydrodeoxygenation of the oxygenated and unsaturated compounds present in the feed.

The `HYDRO-R` unit was modeled in Aspen Plus as an `RYield` reactor, converting the decomposed organic mixture and hydrogen into a combination of liquid hydrocarbons and gaseous by-products. The overall yield distribution implemented in the model and the corresponding output mass flow (kg/hr) is summarized in Table 5.4. The yield fractions were determined by combining the decomposition data provided by BETO [100] with the carbon number distribution extracted from the literature (Figure 2.3). The mass contribution of each carbon chain (C_7–C_{17}) was estimated from the referenced composition profile and normalized to represent approximately 80 % of the total yield, while the remaining 20 % corresponds to water, carbon dioxide, carbon monoxide, hydrogen, and light hydrocarbons (C_4–C_6) generated as secondary hydrogenation products.

Table 5.4: Overall yield distribution defined in the Aspen Plus `HYDRO-R` reactor.

Component	**Yield** [-]	**Mass Flow (kg/hr)**
H_2O	0.050	38.0
CO_2	0.040	30.41
CO	0.003	2.28
H_2	0.007	5.32
CH_4	0.100	76.
C_4	0.001	0.76
C_5	0.001	0.76
C_6	0.001	0.76
C_7	0.010	7.60
C_8	0.0406	30.86
C_9	0.0947	71.99
C_{10}	0.1484	112.82
C_{11}	0.1784	135.63
C_{12}	0.1462	111.15
C_{13}	0.0933	70.93
C_{14}	0.0510	38.77
C_{15}	0.0224	17.03
C_{16}	0.0110	8.36
C_{17}	0.0010	0.76
Total	**1.000**	**764.41**

The simulated yield distribution reproduces the typical bell shaped carbon profile characteristic of upgraded HTL oils and Jet fuels, with a dominant production of mid range hydrocarbons (C_{10}–C_{12}) [95] [100]. The lighter gases CH_4, CO, and CO_2 result primarily from cracking, methanation, and hydrodeoxygenation reactions, while the moderate H_2O formation confirms the effective removal of oxygen from the feedstock. From the decomposer, the stream enters a cooler where the stream is cooled down to 10 °C.

5.5. Upgrading Phase

The upgrading phase represents the final step of the overall simulation, converting the hydrotreated effluent into a refined jet fuel fraction and isolating gaseous by-products. Figure 5.6 illustrates the full process configuration, consisting of a three phase separator (3P-SEP2), a pressure reduction valve, two phase separator (2P-SEP2), two distillation columns (DIST-1 and DIST-2), and a final gas clean up and carbon capture unit (CO2-CAP).

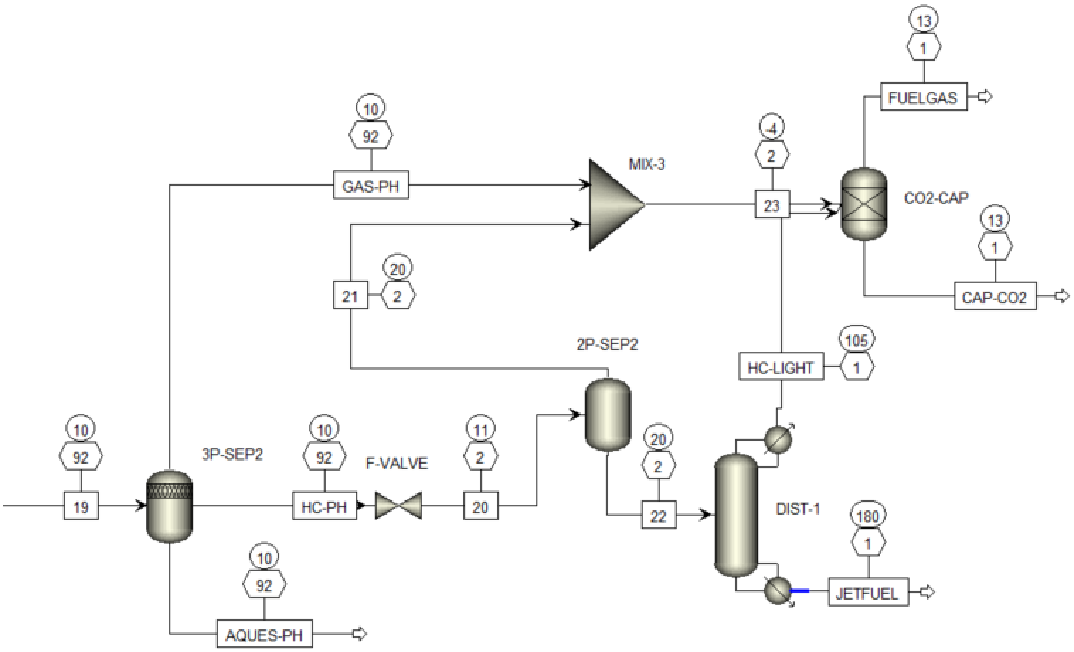

Figure 5.6: Flowsheet of the upgrading phase simulation in Aspen Plus.

5.5.1. Three Phase Separation (3P-SEP2)

The hydrotreated mixture exiting the cooler at 10,°C and 92,bar enters a three-phase separator. The aqueous phase, composed primarily of water with trace amounts of dissolved gases and light hydrocarbons, is purged at approximately 38.15,kg/hr. Since this stream is minimal and not subjected to any downstream valorization, no dedicated pressure-reducing valve was incorporated prior to discharge. The remaining hydrocarbon and gaseous phases proceed to subsequent separation and fractionation stages.

Table 5.5: Summary of 3P-SEP2 outlet streams.

Stream	Description	Phase	Mass Flow (kg/h)
AQUES-PH	Aqueous phase	Liquid	37.94
HC-PH	Hydrocarbon phase	Liquid	648.28
GAS-PH	Light gases	Vapor	74.04

5.5.2. Two Phase Separator (2P-SEP2)

The hydrocarbon phase (HC-PH) undergoes depressurization from 92 bars to 2 bars through a throttling valve (F-VALVE), and then enters a two phase separator. The flashed gases (mainly CO_2 and CH_4, H_2 and CO) are directed to the gas treatment route, while the liquid phase is sent to the primary distillation column (DIST-1). Table 5.6 summarizes the stream distributions.

Table 5.6: Summary of 2P-SEP2 outlet streams.

Stream	Description	Phase	Mass Flow (kg/h)
21	Gas phase	Vapour	39.39
22	Hydrocarbon phase	Liquid	608.89

5.5.3. Primary Distillation

The final upgrading stage begins with the atmospheric distillation column (`DIST-1`), designed to fractionate the hydrotreated mixture into a light gaseous overhead stream and a liquid hydrocarbon product within the kerosene boiling range. The column operates at 1 bar and comprises ten theoretical stages, with a controlled distillate rate of 19.35 kg/hr. The feed enters at 20 °C with a total mass flow of 928.4 kg/hr. This configuration ensures that the resulting bottom product (`JETFUEL`) corresponds to the jet fuel boiling interval defined by the

BETO kerosene curve [100], while minimizing losses of mid range hydrocarbons to the vapor phase. As summarized in Table 5.7, the overhead stream (`HC-LIGHT`) primarily contains low molecular weight hydrocarbons up to C_7, whereas the liquid product (`JETFUEL`) is dominated by paraffinic compounds in the C_8–C_{16} range, confirming effective fractionation within the targeted kerosene cut.

Table 5.7: Component flowrates in `DIST-1` outlet streams.

Component	HC-LIGHT (kg/h)	JETFUEL (kg/h)
H_2O	0.0345	2.31×10^{-10}
CO_2	1.243	2.30×10^{-9}
CH_4	0.251	2.37×10^{-11}
H_2	9.07×10^{-5}	2.46×10^{-17}
CO	0.00133	6.15×10^{-15}
C_4	0.483	4.62×10^{-6}
C_5	0.660	0.000166
C_6	0.725	0.00427
C_7	6.671	0.828
C_8	8.321	22.411
C_9	0.933	70.958
C_{10}	0.0262	112.737
C_{11}	0.000753	135.603
C_{12}	1.05×10^{-5}	111.143
C_{13}	8.26×10^{-8}	70.931
C_{14}	4.62×10^{-10}	38.773
C_{15}	8.50×10^{-12}	17.030
C_{16}	2.05×10^{-13}	8.363
C_{17}	3.84×10^{-16}	0.760

The liquid bottoms stream (`JETFUEL`) from `DIST-1` represents the final upgraded hydrocarbon product, with a mass flow of 589.542,kg/h

Overhead Stream and CO_2 Capture Cycle

The overhead stream (`HC-LIGHT`) leaving `DIST-1` consists primarily of light hydrocarbons between C_4 and C_7, accompanied by non condensable gases such as CO_2 and CH_4. These components form the gaseous fraction of the upgrading system and are directed to the CO_2 capture subsystem (`CO2-CAP`). To simplify the process representation, the gaseous effluents from the upstream `3P-SEP2` and `2P-SEP2` units are first combined in a mixer (`MIX-3`) before entering `CO2-CAP`, while the `HC-LIGHT` stream from `DIST-1` is directly connected to the capture unit.

In this study, the CO_2 capture system is modelled as an externally provided service operated by a specialised third party company. Under this contractual arrangement, the external operator retains ownership of the captured CO_2 and supplies the upgraded methane rich gas stream back to the process boundary as revenue generating output. This assumption eliminates the need to model the internals of the capture technology, substantially reduces the capital expenditure attributed to the pathway, and streamlines the simulation framework by representing CO_2 removal as a black box separation stage.

Table 5.8: Composition of CO_2-CAP outlet streams (3 s.f.).

Component	CAP-CO2 (kg/h)	FUELGAS (kg/h)
H_2O	0.0681	0
CO_2	30.4	0
CO	2.28	0
CH_4	0	76.02
H_2	0	5.32
Trace hydrocarbons (C_4–C_{17})	18.67	0
Total	**51.4**	**81.3**

The total inlet flow to `CO2-CAP` is 133.5,kg/h, yielding 51.4,kg/h of captured gases and 81.3,kg/h of fuel gas composed primarily of methane with a minor hydrogen fraction. The captured stream represents approximately 38.7 % of the inlet flow, consistent with the removal requirements assumed for the external CO_2 capture service. The recovered fuel gas is returned to the process boundary as a renewable biogas product, contributing positively to the economic performance of the HTL upgrading pathway and aligning with the externalised capture service model adopted in this work.

5.6. Economical Analysis

As the hydrothermal liquefaction (HTL) experiments were conducted at laboratory scale and half of the process was performed via a simulation, the resulting cost figures are not representative of the industrial scale operation. To ensure a valid comparison with the biorefinery pathway, economic assessment for the HTL process and upgrading unit was carried out using the Aspen Process Economic Analyzer (APEA).

This tool provides a comprehensive estimation of capital and operational costs based on the process flowsheet and design parameters simulated in Aspen Plus. However, it must be acknowledged that such estimates carry inherent uncertainties as they are dependent on general cost correlations and market assumptions. Changes in the prices of raw materials, equipment scalling effects, and localized market dynamics can actually change the final capital and operational costs to a significant extent.

5.6.1. CAPEX

To enable a consistent and fair comparison between the two pathways, certain capital expenditure costs from the Biorefinería Zambrana case were also incorporated into the HTL pathway analysis. Specifically, the costs associated with Land and natural goods and Technical installations were included, as these represent common infrastructure and site development requirements that would similarly apply to an industrial scale HTL facility.

Table 5.9: Capital expenditure (CAPEX) cost breakdown for the HTL pathway estimated with Aspen Process Economic Analyzer.

Equipment	Description	Cost [€]
C-1	Compressor	10,406
HEX	Heat Exchanger	370,832
HYDRO-R	Hydrotreater Reactor	20,382
P-1	Pump	442,212
DECOMP-R	Decomposition Reactor	20,554
CO2-CAP	CO_2 Capture Unit	14,706
DIST-1	Atmospheric Distillation Column	61,920
SEP-01	Flash Separator	15,136
HVYDIST	Heavy Distillation Column	149,296
3P-SEP2	Three Phase Separator	29,240
SOLID-S	Solid Separator	18,834
2P-SEP2	Two Phase Separator	14,706
3P-SEP	Three Phase Separator	15,136
HTL-R	HTL Reactor	193,156
C-3	Compressor	12,900
Land and natural goods [9]	Site and infrastructure preparation	12,313,725
Technical installations [9]	Electrical, piping, and civil works	1,389,540
Total CAPEX		**15,082,721**

5.6.2. OPEX

Operational expenditures (OPEX) account for the recurring costs associated with the continuous operation of the HTL upgrading facility. These include utilities such as process water, electricity, steam, and refrigerant consumption, as well as the supply of external hydrogen for hydrotreating reactions. A breakdown of the Operational expenditures can be found on table 5.10.

Table 5.10: Updated operational expenditure (OPEX) breakdown for the HTL pathway under different hydrogen cost scenarios.

Source	Utility	Flow [kg/h]	Flow [kg/yr]	Price	Unit	Total Expense [€]
[109]	Water	8,056	38,668,800	1.47	€/m^3	€ 56,843.14
[120]	H_2 (4.1 €/kg)	700	3,360,000	4.10	€/kg	13,776,000.00
[120]	**H_2 (7.1 €/kg)**	700	3,360,000	7.10	€/kg	23,856,000.00
[120]	H_2 (16.1 €/kg)	700	3,360,000	16.10	€/kg	54,096,000.00
[121]	Electricity	296.54	1,423,402	0.117	€/kWh	166,537.99
Aspen	Cooling agent	13.87	66,586	1.538	€/h	102,397.65
Aspen	Process steam (100 psi)	0.025	119.55	1.267	€/h	151.43
Aspen	Process steam (165 psi)	0.273	1,310.71	3.391	€/h	4,444.36
	Total OPEX (base case)					**€24,186,374.56**

Among these factors, hydrogen procurement represents the single largest operating expense, with market prices reported between 4.1 €/kg and 16.1 €/kg depending on production pathways and supply conditions [120]. For this assessment, an average industrial price of 7.1 €/kg was selected as the base case, resulting in an estimated annual operating cost of approximately €24.8 million. It is important to note that hydrogen price fluctuations within the identified range could shift the total OPEX by more than €20 million, underscoring the dominant influence of hydrogen availability and cost on the economic viability of the HTL pathway

5.6.3. Revenue

The revenue stream for the HTL pathway consists of three primary product outputs: biochar, biogas, and Sustainable Aviation Fuel (SAF). The biochar, a carbon rich solid residue is valued at approximately €800 per tonne [122]. The biogas, mainly composed of methane, was valued at €1.25 per kilogram based on an equivalent market rate of €90/MWh for biomethane [123]. The main economic driver of the process is the production of SAF, with an estimated market price of €2,085 per tonne according to EASA's 2024 benchmark for biofuel derived aviation fuels [124]. Combining all product streams, the total annual revenue for the HTL pathway is estimated at **€9.95 million per year**. A breakdown of production mass flows and revenues of each stream can be found in table 5.11.

Table 5.11: Annual revenue breakdown for the HTL pathway based on product output and 2024 market prices.

Source	Flow [kg/h]	Flow [kg/yr]	Price	Unit	Total Revenue [€]
Biochar	927.63	4,452,645.53	800	€/tonne	3,562,116.43
Biogas	81.34	390,475.72	1.25	€/kg	488,094.65
SAF	589.54	2,829,800.91	2,085	€/tonne	5,900,134.89
Total Annual Revenue					**€9,950,345.97**

Chapter 6

Result Analysis

6.1. Bio Ethanol Pathway Results: Yields, Byproducts & Financial analysis

Biorefinerías Zambrana operates an integrated biorefinery designed to valorize multiple winery residues into bio-based products. The primary material inputs to the process are grape pomace (29,000 t/year), wine lees (6,667 t/year), surplus wine (4,000 t/year), polyphenol-rich extracts (3,600 t/year), and non-alcoholic wine fractions (200 t/year).

The detailed list of product streams, including annual quantities, unit prices, and total revenues, was presented previously in Table 3.3. To complement this, Figure 6.1 provides a visual representation of the revenue distribution across the main product categories.

The results indicate that **bioethanol**, **tartaric acid**, and **polyphenolic extracts** are the principal revenue drivers, collectively accounting for more than 80 percent of total annual income. Additional contributions arise from alcohol-free wine and biomass residues, while pigments such as enocyanins generate smaller but still valuable niche revenues. Altogether, the portfolio of products and by-products yields a total annual revenue of **21.66 million euros**.

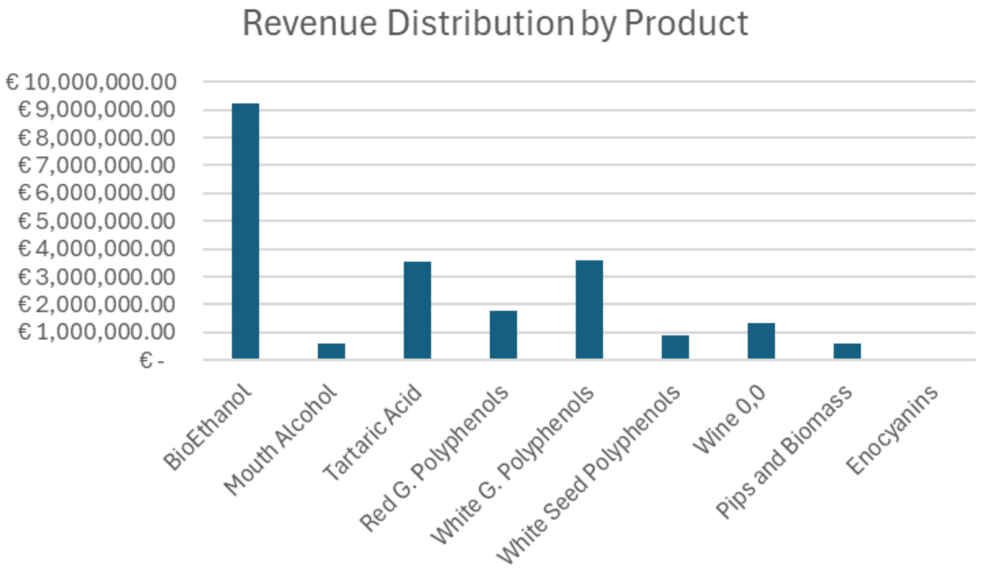

Figure 6.1: Revenue distribution by product for the Biorefinerías Zambrana pathway

The total capital expenditure (CAPEX) of the facility is estimated at approximately €32.94 million, while the operational expenditure (OPEX) amounts to €0.82 million per year. The largest share of CAPEX corresponds to machinery and land acquisition, which is typical of industrial scale bioprocessing facilities. Electricity represents the main component of OPEX, followed by water and reagent consumption, as detailed in table 3.2. Figure 6.2 summarizes the costs by the Zambrana Pathway.

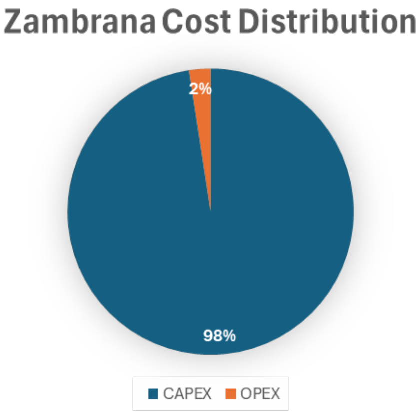

Figure 6.2: Cost Distribution for Zambrana Pathway

Based on the revenue streams obtained, it is evident that the Zambrana biorefinery operates under a highly favorable economic balance. With a total annual revenue of approximately €21.66 million and an OPEX of only €0.82 million, the process generates nearly **26 times more revenue than its annual operating costs**. It is important to note, however, that personnel and administrative salaries have not been included in this preliminary assessment, meaning that the actual operating expenses would be moderately higher in a complete financial evaluation. However, even when accounting for these additional costs, the strong revenue margin indicates that the plant is capable of covering its operational expenditures while achieving financial self sufficiency within the early years of operation.

6.2. HTL Pathway Results: Yields, By-products, and Financial Analysis

The hydrothermal liquefaction (HTL) pathway was modelled to evaluate the conversion of grape pomace into sustainable aviation fuel (SAF) and complementary by-products such as biochar and biogas. The design and economic evaluation were performed using Aspen Plus and the Aspen Process Economic Analyzer (APEA), respectively.

The simulation results indicate that the system produces three marketable output streams: biochar, biogas (mainly composed of CH_4), and SAF. These products represent distinct market opportunities, contributing to the circularity and overall profitability of the HTL process. The detailed revenue estimate for each product was previously presented in Table 5.11. Figure 6.3 summarizes the distribution of annual revenues between the three product streams.

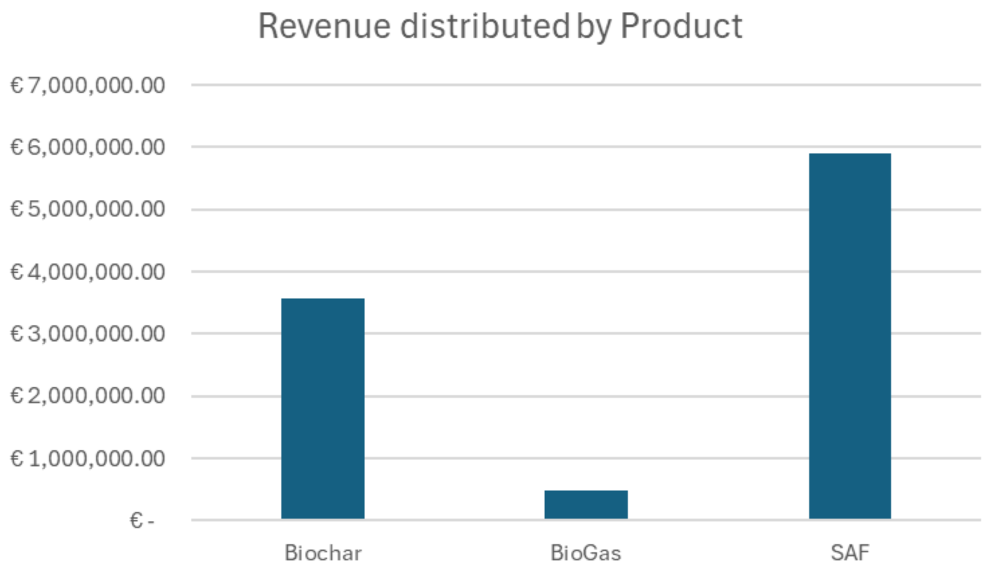

Figure 6.3: Revenue distribution by product for the HTL pathway

The total capital expenditure (CAPEX) estimated through the APEA amounts to approximately €15.08 million, including site and infrastructure costs adapted from Biorefinerías Zambrana. The annual operational expenditure (OPEX) is estimated at €24.18 million, primarily driven by hydrogen supply, which accounts for over 95% of the total operating cost. With an annual revenue of approximately €9.95 million, the process currently operates **below economic breakeven**, highlighting the sensitivity of profitability to hydrogen market prices. Chart 6.4 represents the cost distribution for the HTL pathway.

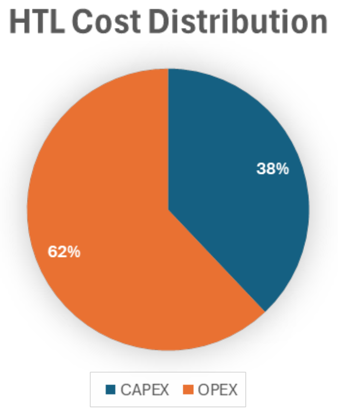

Figure 6.4: Cost Distribution for HTL Pathway

If hydrogen costs were to decrease to around €4.1/kg, as projected under future large scale renewable hydrogen scenarios, total OPEX would fall significantly, improving the economic outlook of the HTL pathway [120]. This underlines the strong dependence of thermochemical upgrading processes on low cost hydrogen availability. Despite this limitation, the HTL route demonstrates technical viability and flexibility in valorizing winery residues into advanced biofuels and carbon based co-products.

6.3. Comparative Analysis of the Bioethanol and HTL Pathways

To assess the techno-economic performance of both studied routes, a comparative analysis was conducted between the Biorefinerías Zambrana (bioethanol) pathway and the Hydrothermal Liquefaction (HTL) pathway. Table 6.1 summarizes the production quantities and revenues associated with the main products and by-products of each process.

Table 6.1: Comparison of production quantities and revenues between the two pathways.

Product Type	**Zambrana (Bioethanol)**		**HTL (SAF)**	
	Quantity (kg/year)	**Revenue (€)**	**Quantity (kg/year)**	**Revenue (€)**
Primary Product	3,076,857	€ 9,230,571	2,829,801	€ 5,900,135
By-products (combined)	7,228,410	€ 12,434,182	4,843,121	€ 4,050,211
Total Annual Revenue		**€ 21,664,753**		**€ 9,950,346**

The results indicate that the Biorefinerías Zambrana pathway achieves a higher overall production and revenue compared to the HTL route. In terms of primary product, Zambrana produces approximately 3.1 million kg of bioethanol per year, while the HTL process yields around 2.8 million kg of sustainable aviation fuel (SAF). Despite the relatively similar production scale, the difference in market price results in a primary product revenue of €9.23 million for bioethanol versus €5.9 million for SAF.

The disparity becomes more pronounced when examining the by-products. The Zambrana pathway generates a diverse portfolio of secondary outputs; including tartaric acid, polyphenolic extracts, and biomass residues, amounting to nearly 12 million kg per year and €12.43 million in additional revenue. In contrast, the HTL route produces only about 5.1 million units of co-products (biochar and biogas) with a combined revenue of €4.30 million. This difference can be partly attributed to the broader feedstock base of the Zambrana facility, which incorporates multiple input streams such as white pomace, wine lees, polyphenols, and unsold wine.

Nevertheless, when comparing only the primary feedstock, red grape pomace, the performance gap narrows, as both systems rely on similar carbon sources and conversion efficiencies. This reinforces the idea that Zambrana's superior economic performance arises mainly from its multiproduct integration rather than from higher yields within a single conversion route. In contrast, the HTL process focuses on producing a single high value fuel with substantial future potential under decarbonization frameworks, suggesting that its profitability could improve significantly under favorable policy and hydrogen cost conditions.

6.3.1. CAPEX and OPEX Comparison

As shown in Figure 6.5, both pathways present comparable capital investment requirements, with estimated CAPEX values of approximately €32.94 million for the Biorefinerías Zambrana bioethanol plant and €15.08 million for the HTL system. The difference arises mainly from the level of process integration and the number of operational units: Zambrana's multiproduct facility requires extensive separation and purification infrastructure, while the HTL system is characterized by fewer but more specialized high pressure units.

As discussed previously, the main drawback of the HTL pathway lies in its high operational expenditure, largely driven by hydrogen consumption. While both pathways require a comparable level of capital investment, the Zambrana biorefinery maintains substantially lower annual operating costs, resulting in a more favorable balance between CAPEX, OPEX, and revenue generation.

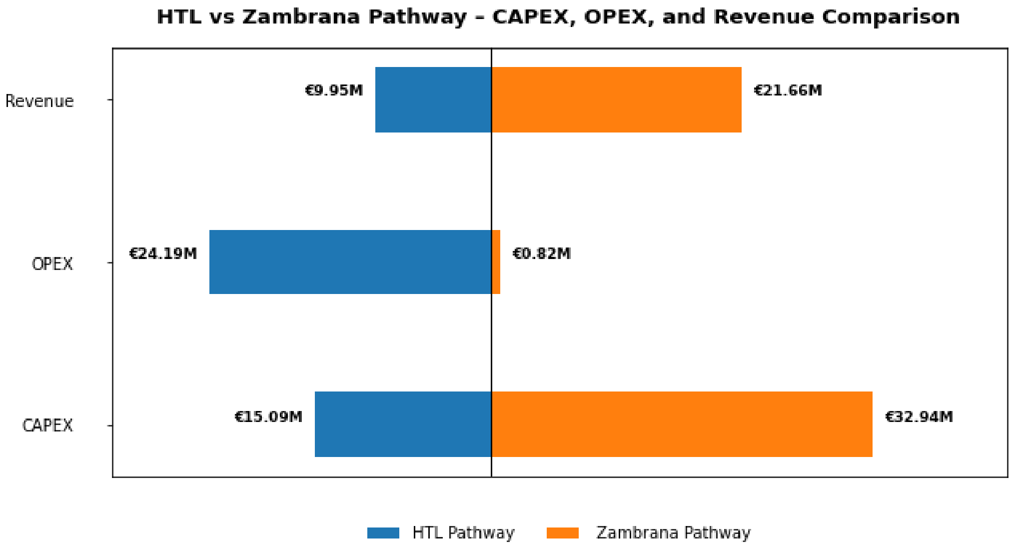

Figure 6.5: Comparison of CAPEX, OPEX, and annual revenue between the Biorefinerías Zambrana and HTL pathways.

Figure 6.5 graphically compares both pathways in terms of CAPEX, OPEX, and annual revenues. The results clearly illustrate that while the Zambrana process maintains a favorable balance between investment, operation, and income, the HTL pathway remains economically constrained under current hydrogen market conditions.

Chapter 7

Conclusions and Recommendations

7.1. Summary of Findings

In summary, the comparative assessment indicates that the Biorefinerías Zambrana pathway is currently the most economically sustainable option. Its multiproduct configuration enables financial self-sufficiency with comparatively low operational costs. By contrast, the HTL pathway, despite its technological viability and its capacity to produce drop-in Sustainable Aviation Fuel, is constrained by the high cost of hydrogen, which prevents it from achieving competitiveness under present market conditions. Nevertheless, the long-term prospects of HTL remain strategically significant. As renewable hydrogen becomes more affordable and as regulatory frameworks increasingly promote low-carbon aviation fuels, the HTL route could develop into a viable and complementary option within future decarbonized fuel systems.

7.2. Recommendations for Industry and Policymakers

To enable the large scale deployment of hydrothermal liquefaction (HTL) and fermentation pathways for grape pomace valorization (and lignocellulosic residues more broadly), the regulatory and policy framework must evolve. The following sections summarize the current situation in Spain and the European Union and propose improvements for each regulatory area.

1. Eligibility and Classification of Biomass Feedstocks

Current situation:

Under the European Union Renewable Energy Directive (RED II, Directive 2018/2001), certain waste and residue feedstocks are listed in Annex IX Part A as eligible for advanced biofuels, which allows for favourable accounting mechanisms such as double counting for compliance purposes. Notably, grape marcs and wine lees are explicitly included in this annex. Spain transposed key provisions through national regulation. The contractual framework and traceability requirements for advanced biofuels were reinforced under Royal Decree 235/2018 and amendments to Royal Decree 1597/2011, which define eligible raw material categories and introduce digital verification of feedstock origin. Spanish regulatory oversight bodies, including the CNMC, have recently strengthened verification rules to improve transparency and mitigate fraud.

Recommended improvements:

- Encourage periodic updates of Annex IX feedstock lists to incorporate new agri-food residues from the wine industry, supported by clear sustainability criteria.
- Harmonise Spanish waste legislation with the EU's "secondary raw material" classification to avoid treating grape pomace as waste, thereby reducing permitting and transport constraints.
- Enable collective certification schemes for small wineries, allowing them to pool feedstocks under unified verification systems and reduce administrative burden.
- Establish clearer long-term investment signals for advanced biofuels through stable minimum-price support mechanisms or guaranteed offtake agreements for Annex IX products, reducing investor uncertainty.
- Introduce a differentiated hydrogen certification framework that recognises the use of renewable hydrogen in upgrading processes such as HTL, enabling these pathways to benefit more effectively from EU RFNBO incentives.
- Promote regional aggregation centres for winery residues to improve logistics efficiency, reduce transport emissions, and stabilise feedstock supply for industrial biorefineries.
- Expand national funding programmes for pilot-scale thermochemical platforms, including HTL, pyrolysis, and gasification, to accelerate the commercial readiness of SAF-oriented technologies.

2. Permitting, Emissions, and Industrial Regulation

Current situation:

Biofuel and biorefinery installations in the European Union fall under the scope of the Industrial Emissions Directive (IED, 2010/75/EU, amended by Directive (EU) 2024/1785) and must comply with the corresponding Best Available Techniques (BAT) requirements developed through the Sevilla Process. In Spain, Law 7/2022 on Waste and Contaminated Soils further aligns national environmental regulation with the EU Circular Economy Action Plan [125].

Despite this regulatory framework, no BAT reference documents or explicit permitting routes currently exist for hydrothermal liquefaction (HTL) facilities. HTL processes exhibit distinct emissions, effluent characteristics, and operational profiles compared with conventional thermochemical or fermentation based biofuel plants, creating uncertainty for operators and permitting authorities.

Recommended improvements:

- Develop specific BAT guidance for hydrothermal conversion technologies that accurately reflect their emissions profiles, effluent characteristics, and operational risks, including the management of aqueous phase organics and volatile compounds.
- Establish “bio-innovation zones” in wine-producing regions that provide streamlined permitting procedures, reduced administrative fees, and accelerated approval pathways for biorefineries utilising grape derived residues.
- Encourage the co-location of HTL and fermentation units with wineries or regional waste management hubs to reduce transport costs, enable shared utilities, and improve energy integration.
- Introduce clear regulatory criteria for the discharge, treatment, and valorisation of HTL by-products, particularly the aqueous phase, to support resource recovery over waste disposal.

3. Funding and Scale Up Incentives

Current situation:

The EU supports bio based innovation through programs such as Horizon Europe and the Circular Bio based Europe Joint Undertaking (CBE JU). Nevertheless, Spain lacks dedicated national funding instruments for scaling up small or regional advanced biofuel facilities, and the “valley of death” between demonstration and commercial deployment persists.

Recommended improvements:

- Establish a national **Advanced Biofuel Deployment Fund** offering grants or low interest loans for pilot and first of a kind HTL or fermentation plants, particularly in wine producing regions.
- Create public-private consortia that invest in demonstration plants, sharing financial and technical risks among regional governments, universities, and industry stakeholders.
- Introduce fiscal incentives such as accelerated depreciation or corporate tax credits for companies investing in advanced biofuel infrastructure.

4. Market Demand, Mandates, and Co-product Valorization

Current situation:

The EU’s Renewable Energy Directive II (RED II) requires Member States to achieve at least 3.5 percent advanced biofuels in transport by 2030, supported by intermediate milestones and double counting for Annex IX feedstocks [126]. Spain has transposed these provisions, allowing ethanol produced from grape pomace and wine lees to count double toward its national blending obligations [127].

The recently approved Renewable Energy Directive III (RED III) further raises the renewable energy targets and maintains the eligibility of ethanol derived from winery residues for double counting within the transport sector [128].

Recommended improvements:

- Increase national advanced biofuel blending targets beyond the EU minimum to stimulate stronger domestic demand for residue-based fuels.
- Mandate partial offtake of advanced biofuels by public transport, agricultural, or municipal fleets to ensure a stable baseline market.

- Introduce long-term purchase agreements or price guarantees for advanced biofuels derived from winery residues to reduce investor risk.
- Promote the development of markets for co-products such as biochar, aqueous-phase nutrients, and phenolic extracts through certification schemes, public procurement, and green labelling.
- Ensure that biofuels produced from grape pomace qualify for voluntary carbon credits or low-carbon fuel standards in recognition of their high lifecycle greenhouse gas savings.

7.3. Future Research Directions

Future work should aim to refine the technical, economic, and environmental understanding of grape pomace valorization pathways. In particular, several lines of investigation can further advance the development of HTL-derived biofuels and their integration within circular bioeconomy systems:

- **Optimization of hydrothermal liquefaction parameters:** Future studies should investigate optimal temperature, residence time, and feed–water ratio to maximize biocrude yield and quality. Parametric sensitivity analyses could be combined with kinetic modeling to establish predictive correlations for industrial scale-up.
- **Feedstock variability and compositional influence:** Grape pomace composition is shaped not only by grape cultivar (e.g. Tempranillo, Chardonnay) but also by vinification and processing steps (e.g. maceration time, pressing method, fermentation practices) [129]. Therefore, future research should reproduce the full HTL and upgrading pathway across pomaces originating from different grape varieties and winemaking protocols. This approach would help deconvolute how residual sugars, structural carbohydrates (cellulose, hemicellulose, lignin), phenolic compounds, and proteins affect conversion efficiency, product yields, and fuel properties [129].
- **Biochar revalorization and market potential:** The biochar fraction obtained from HTL should be further studied to explore its physicochemical upgrading, such as activation or functionalization, to enhance its market value. Potential applications include soil amendment, carbon sequestration, heavy metal adsorption, and use as a precursor for advanced carbon materials. A detailed market analysis of these sectors would enable a more accurate estimation of its economic contribution to the process.
- **Valorization of the aqueous phase:** Further research is recommended to characterize and valorize the aqueous co-product, which contains valuable oxygenated organics and nutrients [78]. Potential routes include anaerobic digestion, catalytic reforming to hydrogen, or nutrient recovery for circular bioeconomy applications [78].
- **Catalytic upgrading and refining pathways:** Investigating catalytic hydrotreatment or esterification routes for upgrading HTL biocrude to meet biodiesel or drop-in fuel standards could significantly enhance product quality and compatibility with existing refinery infrastructure.
- **Process integration and heat recovery:** A complete energy integration study, including the design of a heat exchanger network and the utilization of waste heat between HTL and upgrading stages, would improve overall energy efficiency and reduce the carbon footprint of the process.
- **CO_2 capture and carbon valorization:** A dedicated assessment of CO_2 capture from HTL upgrading and hydrotreatment off-gases should be conducted to explore its potential as an additional revenue stream. Future studies could evaluate the technical viability and cost of integrating capture technologies (e.g., amine scrubbing, pressure swing adsorption, membrane separation), followed by the economic value of the captured CO_2 under voluntary carbon-credit markets or emerging low-carbon fuel standards. Scenario analysis should quantify revenues from carbon certificates, CO_2 utilisation pathways, and long-term storage contracts, helping determine whether carbon monetization could significantly offset the operating costs of the HTL pathway.
- **Life cycle assessment (LCA):** Conducting a cradle to gate LCA to quantify greenhouse gas emissions, water footprint, and energy return on investment (EROI) would provide a holistic understanding of the environmental performance of both valorization pathways.
- **Onsite renewable hydrogen production and storage:** Future research should evaluate the techno economic performance of producing hydrogen in house through water electrolysis powered by renewable

electricity. This includes assessing different electrolyzer technologies, sizing strategies, and power supply configurations, as well as the potential role of battery energy storage systems (BESS) to balance the intermittent renewable generation with the continuous hydrogen demand of the HTL upgrading unit. A comparative analysis between market based hydrogen procurement and onsite production, including levelised hydrogen cost, capacity factor constraints, and grid interaction, would clarify under which conditions integrated renewable hydrogen supply can improve the overall viability of the HTL pathway.

Appendix A

Zambrana Process Flow Diagram

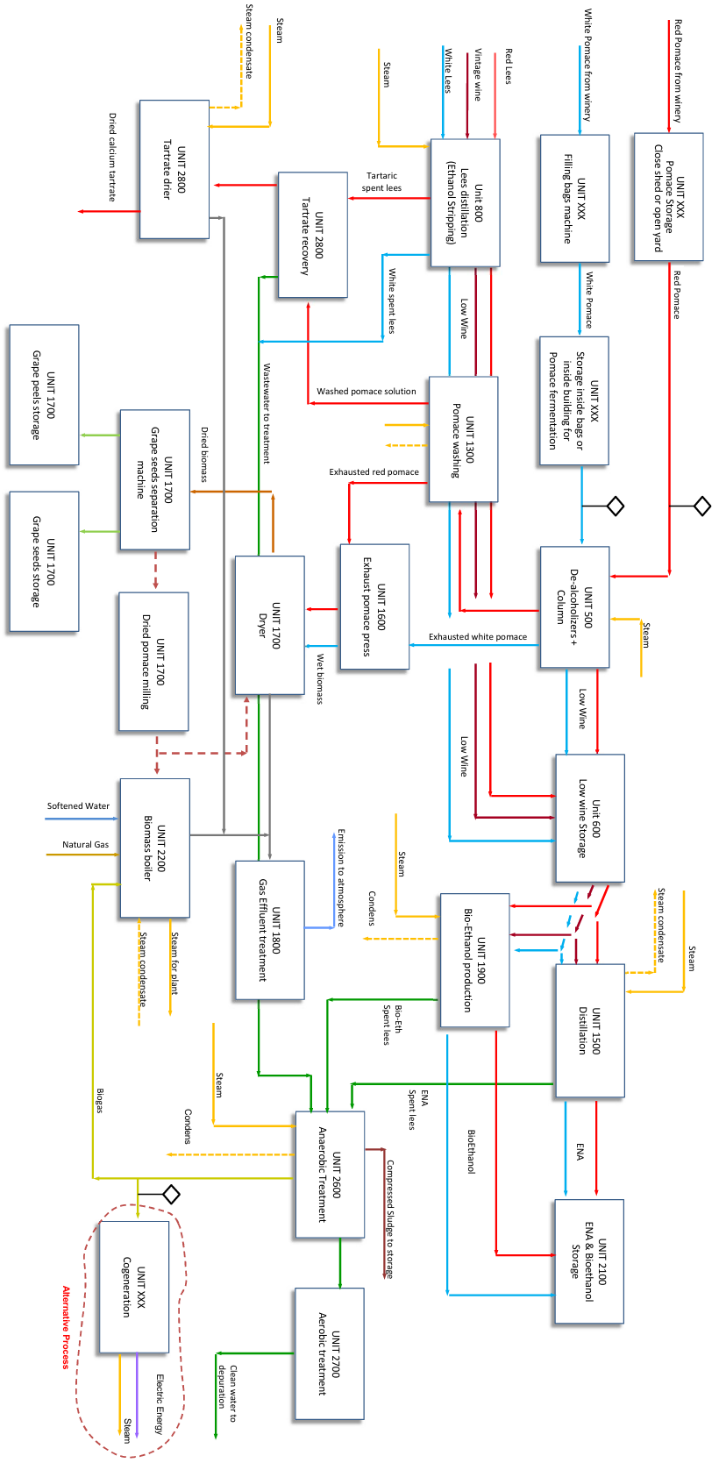

Figure A.1: General process flow diagram of the Zambrana biorefinery. All unit operations (e.g., Unit 500, Unit 1500) are labeled as described in Section **??**.

Appendix B

Full ICP-OES Analysis for Raw biomass, biochar and AQ phase fractions

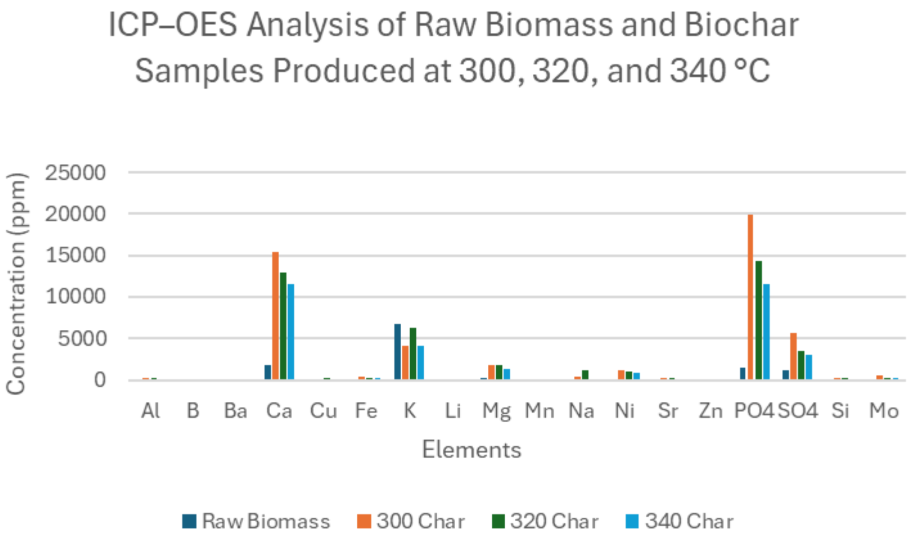

Figure B.1: ICP-OES analysis results for raw biomass and biochar fractions obtained from HTL experiments

Table B.1: ICP-OES analysis results for raw biomass and biochar fractions obtained from HTL experiments.

Element	**Raw Biomass**	**300 °C Char**	**320 °C Char**	**340 °Char**
Al	61	215	212	153
B	20	116	87	54
Ba	2	12	13	8
Ca	1738	15334	12956	11550
Cu	15	81	204	66
Fe	19	359	240	245
K	6682	4059	6320	4080
Li	2	2	44	2
Mg	248	1826	1777	1247
Mn	3	84	41	58
Na	13	369	1127	0
Ni	0	1186	1075	821
Sr	31	226	238	144
Zn	22	53	103	40
PO_4	1479	19917	14309	11593
SO_4	1180	5664	3565	3045
Si	13	205	191	146
Mo	1	530	247	277

All concentrations in [ppm] = [mg/kg].

Table B.2: ICP-OES analysis results for aqueous fractions obtained from HTL experiments.

Element	**300 °C Aq**	**320 °C Aq**	**340 °C aq**
Al	9	7	21
B	47	63	161
Ba	4	5	5
Ca	2698	1817	888
Cu	3	2	2
Fe	2	1	1
K	96912	121970	140320
Li	3	4	4
Mg	2019	2008	376
Mn	14	3	3
Na	902	1009	1066
Ni	1	0	1
Sr	65	119	79
Zn	5	2	3
PO_4	0	0	0
SO_4	2009	2947	3408
Si	554	253	207
Mo	5	17	383

All concentrations in [ppm] = [mg/kg].

Appendix C

GC-MS identified compounds in HTL biocrude Light Organics

Table C.1: GC-MS identified compounds in HTL biocrude Light Organics (quality ≥ 50).

Compound	Retention Time (min)	Area (%)	Quality (%)
1-Butanol, 3-methyl-	5.3981	5.10	90
1-Butanol, 2-methyl-	5.4717	2.80	80
Toluene	6.0365	3.62	91
Cyclopentanone	6.5283	2.25	50
Pyrazine, methyl-	7.2048	3.16	90
Cyclopentanone, 2-methyl-	7.5696	2.33	90
(R)-(+)-3-Methylcyclopentanone	7.7021	1.46	94
Ethylbenzene	7.9940	2.93	90
Styrene	8.5803	3.16	95
Cyclopentanone, 2,3-dimethyl-	8.6553	1.51	76
Nonane	8.7137	1.96	93
2-Cyclopenten-1-one, 2-methyl-	8.8821	5.06	91
Pyrazine, 2,6-dimethyl-	8.9638	2.65	56
Pyrazine, ethyl-	9.0483	1.68	87
Cyclopentanone, 2-ethyl-	9.4974	4.16	62
1H-Pyrrole, 1-butyl-	9.6349	1.70	53
N-Benzyl-2-phenethylamine	9.7805	2.13	55
Aniline	10.2282	5.53	91
Phenol	10.2634	3.91	90
1-Decene	10.4070	1.60	95
2-Cyclopenten-1-one, 3,4-dimethyl-	10.5057	1.85	55
Decane	10.5528	3.11	91
2-Cyclopenten-1-one, 2,3-dimethyl-	10.5768	3.89	81
Benzene, 1-methyl-3-(1-methylethyl)-	11.0420	2.11	93
2-Cyclopenten-1-one, 2,3-dimethyl-	11.2969	5.87	91
1,1'-Bicyclopentyl	11.4989	1.77	50
Benzene, n-butyl-	11.5784	2.24	90
2-Cyclopenten-1-one, 2,3,4-trimethyl-	11.6909	1.05	91
Aniline, N-methyl-	11.7610	1.04	89
o-Toluidine	11.8668	1.20	53
1-Undecene	12.0812	0.92	95
Phenol, 2-methoxy-	12.1304	5.48	93
Undecane	12.2107	3.19	95
5-Undecene	12.2965	0.58	97
2-Ethyl-3-methylcyclopent-2-en-1-one	12.3475	0.63	87
Benzofuran, 2-methyl-	12.4667	0.07	95
Benzene, 2-ethenyl-1,4-dimethyl-	13.1277	1.36	80
Benzene, pentyl-	13.1891	1.65	91
Dodecane	13.7379	1.82	95
Tridecane	15.1593	0.76	97
Pentadecane	17.7519	0.75	97

Bibliography

[1] M. Geissdoerfer, P. Savaget, N. M. P. Bocken, and E. J. Hultink, “The circular economy – a new sustainability paradigm?” Journal of Cleaner Production, vol. 143, pp. 757–768, 2017. DOI: `10.1016/j.jclepro.2016.12.048`.

[2] E. M. Foundation, Completing the picture: How the circular economy tackles climate change, Accessed: 2025-01-13, 2019. [Online]. Available: `https://ellenmacarthurfoundation.org`.

[3] C. Beres, G. N. S. Costa, I. Cabezudo, et al., “Towards integral utilization of grape pomace from winemaking process: A review,” Waste Management, vol. 68, pp. 581–594, 2017. DOI: `10.1016/j.wasman.2017.07.017`.

[4] M. Provenzano, F. Pacchera, C. Silvestri, and A. Ruggieri, “From vineyard to value: A circular economy approach to viticulture waste,” Resources, vol. 13, no. 12, p. 172, 2024.

[5] I. O. of Vine and W. (OIV), State of the world vine and wine sector 2023, Accessed: 2025-01-13, 2023. [Online]. Available: `https://www.oiv.int/sites/default/files/202404/OIV_STATE_OF_THE_WORLD_VINE_AND_WINE_SECTOR_IN_2023.pdf`.

[6] I. O. of Vine and Wine, “State of the world vine and wine sector in 2024,” OIV, 2024.

[7] D. Duca et al., “Analysis of the characteristics of the residues of the wine production chain finalized to their industrial and energy recovery,” Journal of Agricultural Engineering, vol. 44, no. s2, e125, 2013. DOI: `10.4081/jae.2013.s2.e125`.

[8] G. V. Research, Wine market size, share & trends analysis report, Accessed: 2025-01-13, 2021. [Online]. Available: `https://www.grandviewresearch.com/industry-analysis/wine-market`.

[9] Bio - Refinerías Zambrana. [Online]. Available: `https://biozambrana.com/`.

[10] R. Trueman, The World’s 14 Best Wine Regions (When to Visit), 2023.

[11] A. Siller-Sánchez, K. A. Luna-Sánchez, I. Bautista-Hernández, and M. L. Chávez-González, “Use of grape pomace from the wine industry for the extraction of valuable compounds with potential use in the food industry,” Current Food Science and Technology Reports, vol. 2, 2024.

[12] Map of the region of La Rioja, Spain. [Online]. Available: `https://www.mapas.top/espana/mapa-de-la-rioja/`.

[13] La vendimia en La Rioja: curiosidades y tradiciones de la tierra del vino. [Online]. Available: `https://www.vrbo.com/es-es/guias-de-viaje/tipos-de-vacaciones/turismo-gastronomico/la-vendimia-en-la-rioja-cuando-es-y-como-se-trabaja-la-uva`.

[14] E. Commission, A farm to fork strategy for a fair, healthy and environmentally-friendly food system, Accessed: 2025-01-15, 2020. [Online]. Available: `https://ec.europa.eu/food/horizontal-topics/farm-fork-strategy_en`.

[15] G. C. D. Aishi Nath Krishna Das, “Global status of agricultural waste-based industries, challenges, and future prospects,” Agricultural Waste to Value-Added Products, 2023.

[16] C. Toufexis, D.-O. Makris, C. Vlachokostas, A. V. Michailidou, C. Mertzanakis, and A. Vachtsiavanou, “Bridging the gap between biowaste and biomethane production: A systematic review meta-analysis methodological approach,” Sustainability, 2024.

[17] U. Nations, Sustainable development goals: Goal 12 - responsible consumption and production, Accessed: 2025-01-15, 2015. [Online]. Available: `https://sdgs.un.org/goals/goal12`.

[18] A. Zamudio and L. Hernandez, “Anaerobic digestion: Fundamentals, processes, and innovations,” Journal of Bioprocessing, vol. 12, no. 4, pp. 233–245, 2021. DOI: `10.1016/j.jbiopro.2021.08.001`.

[19] Y. Chen and X. Zhang, “Advances in pyrolysis technology for agro-industrial waste management,” Waste Management Journal, vol. 34, pp. 180–195, 2022. DOI: `10.1016/j.wm.2022.03.010`.

[20] R. Kumar and A. Singh, “Enzymatic hydrolysis of agricultural residues for bioethanol production,” Biofuel Research Journal, vol. 17, pp. 134–142, 2020. DOI: `10.1016/j.biores.2020.01.002`.

[21] D. Lin and M. Wei, “Composting agricultural waste: A sustainable practice for soil amendments,” Agronomy Journal, vol. 18, no. 2, pp. 99–112, 2022. DOI: `10.2134/agronj2022.01.01`.

[22] J. Singh and A. Patel, “Biogas production from dairy waste: A technological perspective,” Renewable Energy Journal, vol. 45, pp. 321–332, 2021. DOI: `10.1016/j.renene.2021.05.018`.

[23] R. Garcia and J. Lopez, “Water recycling techniques in agro-industrial processing,” Water Management Review, vol. 29, no. 7, pp. 234–245, 2020. DOI: `10.1016/j.watman.2020.06.009`.

[24] T. Ahmed and C. Brown, “Nutrient recovery from agro-industrial wastewater: Innovations and challenges,” Sustainability Journal, vol. 13, no. 3, pp. 111–124, 2021. DOI: `10.1016/j.sus.2021.03.002`.

[25] P. J. Talboys, J. Heppell, T. Roose, J. R. Healey, D. L. Jones, and P. J. A. Withers, “Struvite: A low-release fertiliser for sustainable phosphorus management?” Plant and Soil, 2015.

[26] S. Jones and R. Miller, “Development of bio-based materials from agricultural residues,” Journal of Materials Research, vol. 42, pp. 222–239, 2023. DOI: `10.1016/j.matres.2023.02.011`.

[27] S. Mehariya et al., “Biorefinery for agro-industrial waste into value-added biopolymers: Production and applications,” Biorefineries: A Step Towards Renewable and Clean Energy, 2021.

[28] M. G. Naitam, G. S. Tomar, R. Kaushik, S. Singh, and L. Nain, “Agro-industrial waste as potential renewable feedstock for biopolymer poly-hydroxyalkanoates (pha) production,” Enzyme Engineering, 2022.

[29] V. Rajput et al., “Biochar production methods and their transformative potential for environmental remediation,” Discover Applied Sciences, 2024.

[30] G. Ravindiran et al., “Production and modifications of biochar to engineered materials and its application for environmental sustainability: A review,” Biochar, 2024.

[31] Y. Li and X. Zhang, “Lignocellulosic biofuels: Advances in production from agricultural waste,” Bioenergy Research, vol. 19, no. 5, pp. 455–470, 2022. DOI: `10.1016/j.biores.2022.05.005`.

[32] J. Lee and S. Park, “Extraction of nutraceuticals from agro-industrial by-products,” Journal of Food Science and Technology, vol. 56, pp. 1331–1345, 2021. DOI: `10.1007/s13197-020-04610-8`.

[33] S. Allaqaband et al., “Utilization of fruit seed-based bioactive compounds for formulating the nutraceuticals and functional food: A review,” Frontiers in Nutrition, vol. 9, 2022.

[34] G. R. Caponio, F. Minervini, G. Tamma, G. Gambacorta, and M. D. Angelis, “Promising application of grape pomace and its agri-food valorization: Source of bioactive molecules with beneficial effects,” Sustainability, vol. 15, no. 11, 2023.

[35] F. M. M. Janice da Conceição Lopes Joana Madureira and S. C. Verde, “Grape pomace: A review of its bioactive phenolic compounds, health benefits, and applications,” Molecules, vol. 30, no. 2, 2023.

[36] E. Lopez and J. Garcia, “A review of circular economy practices in agro-industries,” Journal of Cleaner Production, vol. 312, pp. 127–140, 2021. DOI: `10.1016/j.jclepro.2021.03.004`.

[37] D. C. Elliott, A. J. Schmidt, T. R. Hart, and J. M. Billing, “Conversion of wet waste feedstock to biocrude by hydrothermal processing in a continuous-flow reactor: Grape pomace,” Biomass Conversion and Biorefinery, 2017.

[38] E. M. Tobía, “Producción de biogás y fertilizantes a partir de residuos vitivinicolas mediante digestión anaerobia,” 2019.

[39] R. Sirohia et al., “Green processing and biotechnological potential of grape pomace: Current trends and opportunities for sustainable biorefinery,” Bioresource Technology, 2020.

[40] J. Yu. and M. Ahmedna, “Functional components of grape pomance: Their composition, biological properties and potential applications,” International Journal of Food science and Technology, 2013.

[41] Y. Zheng et al., “Ensilage and bioconversion of grape pomance into fuel ethanol,” Journal of Agricultural and Food Chemistry, 2012.

[42] B. M. da Silva Pedras, “Valorization of grape pomance through hot compressed water extraction/hydrolysis,” Facultad de ciencias e tecnologia - Universidade Nova de Lisboa, 2015.

[43] J. R. Vinyard, C. A. Myers, G. K. Murdoch, P. Rezamand, and G. E. Chibisa, “Optimum grape pomace proportion in feedlot cattle diets: Ruminal fermentation, total tract nutrient digestibility, nitrogen utilization, and blood metabolites,” Journal of Animal Science, vol. 99, no. 2, skab044, 2021. DOI: `10.1093/jas/skab044`.

[44] F. Blasi, V. Trovarelli, L. Mangiapelo, F. Ianni, and L. Cossignani, “Grape pomace for feed enrichment to improve the quality of animal-based foods,” Foods, vol. 13, no. 22, p. 3541, 2024. DOI: `10.3390/foods13223541`.

[45] Grappa.com. “The production of grappa. ”[Online]. Available: `https://www.grappa.com/en/grappa/production/the-production-of-grappa`.

[46] M. Cisneros-Yupanqui, C. Rizzi, D. Mihaylova, and A. Lante, “Effect of the distillation process on polyphenols content of grape pomace,” European Food Research and Technology, vol. 248, pp. 929–935, 2022. DOI: `10.1007/s00217-022-03980-4`. [Online]. Available: `https://doi.org/10.1007/s00217-022-03980-4`.

[47] T. Ahad, D. Majid, S. Naqash, H. A. Makroo, S. J. Rashid, and B. N. Dar, “Exploring bioactive compounds in lyophilized grape pomace extracts: Comparative analysis of traditional and innovative extraction methods,” Journal of Food Measurement and Characterization, 2024.

[48] H. N. Rajha et al., “Extraction of total phenolic compounds, flavonoids, anthocyanins and tannins from grape byproducts by response surface methodology: Influence of solid-liquid ratio, particle size, time, temperature and solvent mixtures on the optimization process,” Food and Nutrition Sciences, 2014.

[49] M. S. K. J, P. R, and P. Panneerselvam, “Hydrothermal liquefaction a sustainable technique for present biofuel generation: Opportunities, challenges and future prospects,” Fuel, vol. 385, 2025.

[50] R. Seiser and H. Wang, Co-processing fast pyrolysis bio-oils and hydrothermal liquefaction biocrudes in fluid catalytic cracking and hydroprocessing in refineries, 2023.

[51] C. Deepika et al., “Hydrothermal liquefaction of wet microalgal biomass for biofuels and platform chemicals: Advances and future prospects,” Discover Applied Sciences, vol. 6, p. 245, 2024.

[52] Department of Energy, Integrated strategies to enable lower-cost biofuels, 2020. [Online]. Available: `https://www.energy.gov/sites/default/files/2020/07/f76/beto-integrated-strategies-to-enable-low-cost-biofuels-july-2020.pdf`.

[53] V. S. Kurćubić et al., “Valorizing grape pomace: A review of applications, nutritional benefits, and potential in functional food development,” Foods, vol. 13, no. 24, p. 4169, 2024. DOI: `10.3390/foods13244169`. [Online]. Available: `https://doi.org/10.3390/foods13244169`.

[54] A. Almanza-Oliveros et al., “Grape pomace—advances in its bioactivity, health benefits, and food applications,” Foods, vol. 13, no. 4, p. 580, 2024. DOI: `10.3390/foods13040580`. [Online]. Available: `https://doi.org/10.3390/foods13040580`.

[55] News-Medical. “Turning wine waste into wellness: Grape pomace’s journey from by-product to superfood. ”[Online]. Available: `https://www.news-medical.net/news/20240215/Turning-wine-waste-into-wellness-Grape-pomaces-journey-from-by-product-to-superfood.aspx`.

[56] M. Mikus and S. Galus, “Biopolymers from agriculture waste and by-products,” Springer Series on Polymer and Composite Materials, 2022.

[57] C. Berger et al., “Production of sustainable polymeric composites using grape pomace biomass,” Biomass Conversion and Biorefinery, vol. 12, pp. 5869–5880, 2020. DOI: `10.1007/s13399-020-00911-8`.

[58] C. Maraveas, “Production of sustainable and biodegradable polymers from agricultural waste,” Polymers, vol. 12, no. 5, p. 1127, 2020. DOI: `10.3390/polym12051127`. [Online]. Available: `https://www.mdpi.com/2073-4360/12/5/1127`.

[59] K. Subramanian and K. Suresh, “Metabolic and biochemical pathways for anaerobic digestion,” Microorganisms for Sustainability, vol. 44, pp. 3–25, 2024.

[60] A. Topaloğlu, Ö. Esen, B. Turanlı-Yıldız, M. Arslan, and Z. P. Çakar, “From saccharomyces cerevisiae to ethanol: Unlocking the power of evolutionary engineering in metabolic engineering applications,” Journal of Fungi, vol. 9, no. 10, p. 984, 2023. DOI: `10.3390/jof9100984`. [Online]. Available: `https://doi.org/10.3390/jof9100984`.

[61] Frontiers in Bioengineering and Biotechnology, “Saccharomyces cerevisiae for lignocellulosic ethanol production: A look at the future,” Bioengineering Biotechnology, 2024. [Online]. Available: `https://www.frontiersin.org/journals/bioengineering-and-biotechnology/articles/10.3389/fbioe.2024.1466644/full`.

[62] BioEnergy Consult, Biomass pyrolysis process, 2023. [Online]. Available: `https://www.bioenergyconsult.com/biomass-pyrolysis-process/`.

[63] X. Cao, S. Sun, and R. Sun, “Application of biochar-based catalysts in biomass upgrading: A review,” RSC Advances, vol. 7, pp. 48 793–48 805, 2017. DOI: `10.1039/C7RA09307A`. [Online]. Available: `https://doi.org/10.1039/C7RA09307A`.

[64] A. I. Osman, N. Mehta, A. M. Elgarahy, A. Al-Hinai, A. H. Al-Muhtaseb, and D. W. Rooney, "Conversion of biomass to biofuels and life cycle assessment: A review," Environmental Chemistry Letters, vol. 19, pp. 4075–4118, 2021. DOI: `10.1007/s10311-021-01273-0`.

[65] R. Jilte, "Stages of biomass gasification and chemical reactions," JETIR, 2023.

[66] EnggCyclopedia, Gasification reactions, 2012. [Online]. Available: `https://enggcyclopedia.com/2012/01/gasification-process-reactions/`.

[67] Global Syngas Technologies Council, Synthetic fuels, 2023. [Online]. Available: `https://globalsyngas.org/syngas-technology/syngas-applications/synthetic-fuels/`.

[68] K. J. Whitty, "Challenges and lessons learned in commercial biomass gasification and co-gasification of waste," in U.S. DOE Workshop, 2022. [Online]. Available: `https://www.energy.gov/sites/default/files/2022-12/beto-06-gasification-wkshp-nov-2022-whitty.pdf`.

[69] C. Manochio, B. Andrade, R. Rodriguez, and B. Moraes, "Ethanol from biomass: A comparative review," Renewable aND Sustanable Energy Reviews, vol. 80, pp. 743–755, 2017.

[70] J. M. Matias, F. Braga, and A. Vilela, "Upcycling wine industry waste: Dealcoholized grape pomace as a platform for bio-based material innovation," Applied Sciences, 2025.

[71] R. R. Díez, "Development of an integrated and green biorefinery from winery waste. application to wine lees and grape stems," PROGRAMA DE DOCTORADO EN INGENIERÍA QUÍMICA Y AMBIENTAL, 2018.

[72] Extra Neutral Alcohol - SASMA. [Online]. Available: `https://sasmabv.com/products/extra-neutral-alcohol/`.

[73] B. Ahmad et al., "Integrated biorefinery approach to valorize winery waste: A review from waste to energy perspectives," Science of the total environment, 2020.

[74] A. A. Peterson, F. Vogel, R. P. Lachance, M. Fröling, M. J. Antal, and J. W. Tester, "Thermochemical biofuel production in hydrothermal media: A review of sub- and supercritical water technologies," Energy & Environmental Science, vol. 1, no. 1, pp. 32–65, 2008. DOI: `10.1039/B810100K`.

[75] S. S. Toor, L. Rosendahl, and A. Rudolf, "Hydrothermal liquefaction of biomass: A review of subcritical water technologies," Energy, vol. 36, no. 5, pp. 2328–2342, 2011. DOI: `10.1016/j.energy.2011.03.013`.

[76] J. Akhtar and N. A. S. Amin, "A review on process conditions for optimum bio-oil yield in hydrothermal liquefaction of biomass," Renewable and Sustainable Energy Reviews, vol. 15, no. 3, pp. 1615–1624, 2011. DOI: `10.1016/j.rser.2010.11.054`.

[77] M. Elhassan, R. Abdullah, M. R. R. Kooh, and Y.-F. C. Chou, "Hydrothermal liquefaction: A technological review on reactor design and operating parameters," Bioresource Technology Reports, 2023.

[78] M. Usman, S. Cheng, S. Boonyubol, and J. S. Cross, "From biomass to biocrude: Innovations in hydrothermal liquefaction and upgrading," Energy conversion and management, 2024.

[79] R. Bao et al., "A review of hydrothermal biomass liquefaction: Operating parameters, reaction mechanism, and bio-oil yields and compositions," Energy & Fuels, vol. 38, no. 10, pp. 8437–8459, 2024.

[80] D. C. Elliott, P. Biller, A. B. Ross, A. J. Schmidt, and S. B. Jones, "Hydrothermal liquefaction of biomass: Developments from batch to continuous process," Bioresource Technology, vol. 178, pp. 147–156, 2015.

[81] K. H. Akkari, M. S. Matta, and T. B. Patrick, "Mass spectral dehydration and decarboxylation in cyclic α-hydroxy acids, alcohols, and carboxylic acids," Bulletin of the Chemical Society of Japan, vol. 54, no. 2, pp. 641–642, 1981.

[82] S. Shekhar, M. E. Hoque, P. K. Bajpai, H. Islam, and B. Sharma, "Chemical upcycling of plastics as a solution to the plastic trash problem for an ideal, circular polymer economy and energy recovery," Environment, Development and Sustainability, vol. 26, pp. 5629–566, 2024.

[83] O. A. Attallah, V. Palkova, and R. Vij, "Single step depolymerization of multiple polyesters in poly (lactic acid) mixed plastics: Process optimization, pure monomers extraction and kinetics evaluation," Journal of Polymers and the Environment, vol. 33, pp. 117–133, 2025.

[84] O. Y. Al-Abbasy, S. A. Younus, A. I. Rashan, and O. A. S. Ahmad, "Maillard reaction: Formation, advantage, disadvantage and control," Food Science and Applied Biotechnology, vol. 7, no. 1, pp. 333–345, 2024.

[85] P. J. Valdez, J. G. Dickinson, and P. E. Savage, “Characterization of product fractions from hydrothermal liquefaction of nannochloropsis sp. and the influence of solvents,” Energy & Fuels, vol. 25, no. 7, pp. 3235–3243, 2011. DOI: `10.1021/ef3004046`.

[86] B. Khiari and M. Jeguirim, “Pyrolysis of grape marc from tunisian wine industry: Feedstock characterization and thermal degradation,” Energies, 2018.

[87] S. R. Diego López Barreiro, U. Hornung, A. Kruse, and W. Prins, “Hydrothermal liquefaction of microalgae: Effect on production yields of the addition of an organic solvent to separate the aqueous phase and the biocrude oil,” Algal Research, vol. 12, pp. 206–2012, 2015.

[88] D. Xu and P. E. Savage, “Characterization of biocrudes recovered with and without solvent after hydrothermal liquefaction of algae,” Algal Research, vol. 6, pp. 1–7, 2014.

[89] Y. Zhu, M. J. Biddy, S. B. Jones, D. C. Elliott, and A. J. Schmidt, “Techno-economical analysis of liquid fuel production from woody biomass via hydrothermal liquefaction (htl) and upgrading,” Applied Energy, vol. 129, pp. 384–394, 2014.

[90] L. Taşeri, M. Gülcü, and T. Aktaş, “Comparison of grape pomace drying using a solar dryer and under open sun conditions,” Viticulture Studies, 2023.

[91] A. Khalangre, A. Mirza, R. Chavan, A. K. Sharma, N. Shaikh, and A. Shabeer, “Drying and degradation kinetics of red grape pomace with special emphasis on degradation of anthocyanins using liquid chromatography–orbitrap–mass spectrometry,” Biomass Conversion and Biorefinery, 2024, Published 26 September 2024. DOI: `10.1007/s13399-024-06170-4`.

[92] T. Munkin, A. Rajendran, V. K. Garlapati, et al., “Analysis of operational issues in hydrothermal liquefaction and hydrothermal gasification of biomass,” Biomass Conversion and Biorefinery, vol. 13, 2021.

[93] A. V. Rajani, “Pg seminar,” in Fertilizer Composition and Application, 2019.

[94] J. S. dos Passos, P. Straka, M. Auersvald, and P. Biller, “Upgrading of hydrothermal liquefaction biocrudes from mono- and co- liquefaction of cow manure and wheat straw through hydrotreating and distillation,” Chemical Engineering Journal, 2023.

[95] M. Usman, S. Cheng, S. Boonyubol, and J. S. Cross, “The future of aviation soars with htl-based saf’s: Exploring potential and overcoming challenges using organic wet feedstocks,” Sustainable Energy Fuels, 2023.

[96] Sustainable aviation fuel (SAF) – specifications and composition. [Online]. Available: `https://www.bp.com/en/global/air-bp/news-and-views/views/saf_specs_and_comparison.html`.

[97] K. Moriarty and R. McCormick, “Sustainable aviation fuel blending and logistics,” National Renewable Energy Laboratory - NREL, 2024.

[98] D. Castello, M. S. Haider, S. Chiaberge, and L. A. Rosendahl, “Understanding catalytic hydrotreating of hydrothermal liquefaction nitrogen-rich biocrude in a two-stage continous hydrotreater,” Chemical Engineering Journal, 2024.

[99] I. E. Association, “Diesel and gasoline,” Technology collaboration programme on Advanced Motor Fuels, 2020.

[100] J. Holladay, Z. Abdullah, and J. Heyne, “Sustainable aviation fuel: Review of technical pathways,” U.S Department of energy, Bioenergy technologies office (BETO), Tech. Rep., 2020.

[101] P. S. .-. C. of Earth and M. Science, “Cut points,” Petroleum Processing, 2023.

[102] H. Maldonado and D. L. Cutz, Standard operational procedure for bio-oil refinement (wet lab, pe department).

[103] R. F. Culmo, “The elemental analysis of various classes of chemical compounds using chn,” PerkinElmer - Elemental Analysis,

[104] K. Świechowski, W. A. Rasaq, S. Stegenta-Dąbrowska, and A. Białowiec, “Characterization of engineered biochar: Proximate analyses, ultimate analyses, physiochemical analyses, surface analyses, and molecular analyses,” Engineered Biochar, 2022.

[105] S. R. Khan, B. Sharma, P. A. Chawla, and R. Bhatia, “Inductively coupled plasma optical emission spectrometry (icp-oes): A powerful analytical technique for elemental analysis,” Food Analytical Methods, 2021.

[106] D. Turner, “Gc-ms principle, intrument and analyses and gc-ms/ms,” Technology Network: Analysis Separations, 2024.

[107] Frilli, “Process description: Bio-ethanol, ena and tartrate from wine residues,” Frilli: Part of Omnia technologies, Tech. Rep., 2025.

[108] Grupo Vento: Diseño y fabricación de maquinaria industrial. [Online]. Available: `https://www.grupovento.com/`.

[109] Price of Water in Madrid. [Online]. Available: `https://tarifasdeagua.es/info/precio/madrid`.

[110] Nitric Acid Price Outlook. [Online]. Available: `https://www.intratec.us/solutions/primary-commodity-prices/commodity/nitric-acid-prices`.

[111] Calcium carbonate prices remain stable across Europe, China and Malaysia in August 2025. [Online]. Available: `https://www.chemanalyst.com/NewsAndDeals/NewsDetails/calcium-carbonate-prices-remain-stable-across-europe-china-and-malaysia-38674`.

[112] Safety in the operation of laboratory reactors and pressure vessels.

[113] Azti - Member of the Vasc research technology alliance. [Online]. Available: `https://www.azti.es/en/`.

[114] H. Maldonado and D. L. Cutz, Standard operational procedure for bio-oil refinement (wet lab, pe department).

[115] T. Aktas, I. S. Dalmis, L. Taseri, and T. Batur, “A comprehensive characterization of biochar derived from grape pomace via fast pyrolysis,” International Journal of Scientific Research in Science, Engineering and Technology, 2024.

[116] S. Mazhkoo et al., “Catalytic hydrothermal liquefaction of grape pomace using ni–zro$_2$–mss and ni–hzsm5 in a water–crude glycerol cosolvent,” ACS Omega, vol. 7, no. 46, pp. 41 991–42 002, 2022.

[117] N. A. Nasir, “Hydrothermal liquefaction of lignocellulosic biomas,” M.S. thesis, The university of Sheffield, 2019.

[118] I. Pavlovič, Ž. Knez, and M. Škerget, “Hydrothermal reactions of agricultural and food processing wastes in sub- and supercritical water: A review of fundamentals, mechanisms, and state of research,” Journal of Agricultural Food Chemistry, 2013.

[119] The engineering toolbox - Hydrocarbons Physical data. [Online]. Available: `https://www.engineeringtoolbox.com/hydrocarbon-boiling-melting-flash-autoignition-point-density-gravity-molweight-d_1966.html`.

[120] Price of Hydrogen in Global Markets. [Online]. Available: `https://observatory.clean-hydrogen.europa.eu/hydrogen-landscape/production-trade-and-cost/cost-hydrogen-production`.

[121] Electricity Price today in Spain. [Online]. Available: `https://comparadorluz.com/tarifas/precio-kwh`.

[122] B. Garcia, O. Alves, B. Rijo, G. Lourinho, and C. Nobre, “Biochar: Production, applications, and market prospects in portugal,” environments, 2022.

[123] Trends in Biogas Selling Price Across Different Regions. [Online]. Available: `https://chekvan.com/2025/04/16/trends-in-biogas-selling-price-across-different-regions/`.

[124] E. U. A. S. Agency, “2024 aviation fuels reference prices for refueleu aviation,” European Union Aviation Safety Agency - EASA, Tech. Rep., 2024.

[125] Government of Spain, Law 7/2022 on waste and contaminated soils for a circular economy, Spanish waste and circular economy law aligning national legislation with the EU Circular Economy Action Plan, 2022. [Online]. Available: `https://eur-lex.europa.eu/legal-content/EN/TXT/HTML/?uri=CELEX%3A52022SC0256`.

[126] EPure, Overview of biofuels policies and markets across the eu, Provides an overview of RED II implementation and advanced biofuel targets in EU Member States, 2022. [Online]. Available: `https://www.epure.org/wp-content/uploads/2022/10/221011-DEF-REP-Overview-of-biofuels-policies-and-markets-across-the-EU-October-2022.pdf`.

[127] Foreign Agricultural Service, USDA, Spain: Biofuels policy and market, Summary of Spain’s biofuel regulatory framework and implementation of advanced biofuel incentives, 2020. [Online]. Available: `https://apps.fas.usda.gov/newgainapi/api/Report/DownloadReportByFileName?fileName=Spain+Biofuels+Policy+and+Market_Madrid_Spain_07-24-2020`.

[128] Wine Business, European commission confirms double-counting for ethanol from wine pomace and lees, Confirms RED III maintains double-counting status for ethanol derived from winery residues, 2024. [Online]. Available: `https://www.winebusiness.com/news/article/300306`.

[129] B. de Paula Telini, L. C. Villa, M. H. Vainstein, and F. C. Lopez, “From vineyard to brewery: A review of grape pomace characterization and its potential use to produce low-alcohol beverages,” Fermentation, 2025.